Identification of novel PfEMP1 variants containing domain cassettes 11, 15 and 8 that mediate the *Plasmodium falciparum* virulence-associated rosetting phenotype

Florence McLean[1*], Brian R. Omondi[1*], Nouhoum Diallo[1], Stanley Otoboh[1], Carol Kifude[1], Abdirahman Abdi[2], Rivka Lim[1], Thomas Otto[3], Ashfaq Ghumra[1], J. Alexandra Rowe[1]

[1]Institute of Immunology and Infection Research, School of Biological Sciences, University of Edinburgh, Edinburgh, United Kingdom. [2]KEMRI-Wellcome Laboratories, Kilifi, Kenya. [3]Institute of Infection, Immunity and Inflammation, University of Glasgow, Glasgow, United Kingdom.

Short title: identification of novel PfEMP1 variants that mediate rosetting

*joint first authors

Abstract

Plasmodium falciparum erythrocyte membrane protein 1 (PfEMP1) is a diverse family of variant surface antigens, encoded by *var* genes, that mediates binding of infected erythrocytes to human cells and plays a key role in parasite immune evasion and malaria pathology. The increased availability of parasite genome sequence data has revolutionised the ability to study PfEMP1 diversity across multiple *P. falciparum* isolates. However, making functional sense of genomic data relies on the ability to infer binding phenotype from *var* gene sequence. For *P. falciparum* rosetting, the binding of infected erythrocytes to uninfected erythrocytes, the analysis of *var* gene/PfEMP1 sequences encoding the phenotype is limited, with only eight rosette-mediating PfEMP1 variants described to date. These known rosetting PfEMP1 variants fall into two types, characterised by N-terminal domains known as "domain cassette" 11 (DC11) and DC16. Here we test the hypothesis that DC11 and DC16 are the only PfEMP1 types in the *P. falciparum* genome that mediate rosetting, by examining a set of thirteen recent culture-adapted Kenyan parasite lines. We first analysed the *var* gene/PfEMP1 repertoires of the Kenyan lines and identified an average of three DC11 or DC16 PfEMP1 variants per genotype. *In vitro* rosette selection of the parasite lines yielded four with a high rosette frequency, and analyses of their *var* gene transcription, infected erythrocyte PfEMP1 surface expression, rosette disruption and erythrocyte binding function identified four novel rosette-mediating PfEMP1 variants. Two of these were of the predicted DC11 type (one showing the dual rosetting/IgM-Fc-binding phenotype), whereas two contained DC15 (DBLα1.2-CIDRα1.5b) a PfEMP1 type not previously associated with rosetting. We also showed that a Thai parasite line expressing a DC8-like PfEMP1 binds to erythrocytes to form rosettes. Hence, these data expand current knowledge of rosetting mechanisms and emphasize that the PfEMP1 types mediating rosetting are more diverse than previously recognised.

Author summary

Malaria is an infectious tropical disease caused by the parasite *Plasmodium falciparum* that kills more than half a million people every year, mostly young children in sub-Saharan Africa. Life-threatening episodes of malaria are characterised by huge numbers of parasitised red blood cells in the infected host, many of which bind to blood vessel walls and block blood flow, causing tissue damage and organ failure. Sometimes parasitised red cells also bind to uninfected red cells to form clusters of cells called rosettes, which make the blockage of blood flow in vital organs even worse. Previous research has begun to decipher how parasitised red cells bind to uninfected red cells to form rosettes, but little is yet known about the process. Here we identify some new versions of the "sticky proteins" (adhesion molecules) that are made by malaria parasites and displayed on the surface of infected red cells to bring about rosette formation. The rosette-mediating adhesion molecules are members of a large family, and we identify here a few characteristic types within this family that mediate rosetting. This work is an important step towards the goal of understanding how malaria parasite rosettes form rosettes in order to develop preventions or treatments to reverse rosetting and reduce the number of people dying from severe malaria.

56 **Introduction**

57 Rosetting is the binding of erythrocytes parasitised with *Plasmodium spp.* to uninfected erythrocytes
58 during the asexual blood stage of malaria infection, and has been described for *P. falciparum*, *P. vivax*,
59 *P. ovale* and *P. malariae*, as well as in murine and primate malaria parasite species (reviewed by (1)).
60 Rosetting is a phenotypically variable property, with different parasite isolates having between zero
61 and >90% of mature-infected erythrocytes in rosettes (2). The rosetting phenotype is of particular
62 interest in *P. falciparum* malaria, because studies in Sub-Saharan Africa have consistently shown that
63 parasite isolates from severe malaria cases have significantly higher levels of rosetting than those from
64 uncomplicated malaria cases (2-5), raising the possibility that rosetting contributes to disease
65 pathogenesis. Subsequent work has shown that rosettes are stable under physiological blood flow
66 shear forces and enhance microvascular obstruction caused by the sequestration of infected
67 erythrocytes (6-9). Furthermore, human erythrocyte polymorphisms that reduce the ability of *P.*
68 *falciparum* to form rosettes, such as blood group O and the Complement Receptor One (CR1)-related
69 Knops blood group, have been selected to a high frequency in malaria endemic regions and are
70 associated with significant protection against severe disease (10-12), supporting the hypothesis that
71 rosetting is a parasite virulence-associated phenotype.

72 Rosetting in *P. falciparum* infected erythrocytes begins at ~16-20 hours post invasion, a time-
73 point corresponding to the appearance of parasite-derived variant antigens on the infected
74 erythrocyte surface (13). Specific members of the variant surface antigen family *P. falciparum*
75 Erythrocyte Membrane Protein 1 (PfEMP1) are the best characterised rosette-mediating parasite
76 adhesion molecules in *P. falciparum* (14-17), although there is some limited evidence to suggest that
77 other VSA families such as the RIFINs and STEVORs may contribute to rosetting in some parasite
78 genotypes (18, 19). PfEMP1 is encoded by *var* genes that can be classified into three main groups A,
79 B and C and two intermediate groups B/A and B/C by their conserved upstream promoter sequences
80 (20). These groups have functional significance as parasite isolates causing severe malaria
81 predominantly transcribe group A and B/A *var* genes (21-25). PfEMP1 variants have an N-terminal

82 'head structure' composed of an N-terminal sequence (NTS) and Duffy Binding Like (DBL) domain
83 followed by a Cysteine-rich InterDomain Region (CIDR)(26). Downstream from the head structure, a
84 variable number of further DBL and CIDR domains comprise the rest of the extracellular region.
85 PfEMP1 DBL and CIDR domains have been classified using phylogenetic methods into seven (α, β, γ,
86 δ, ε, ζ and pam) and five (α, β, γ, δ and pam) main classes respectively (26), which can be further
87 divided into numerical subclasses (27). Group A *var* genes encode DBLα1 domains, followed by a
88 CIDRα1 or CIDRβ/γ/δ domain in their head structures, whereas group B and C *var* genes encode DBLα0
89 domains followed by CIDRα2-6 domains (26, 27). Domain subclasses frequently found together in
90 tandem are called domain cassettes (DCs) (27).

91 PfEMP1 groups, domain cassettes and domain subclasses have been linked to specific host
92 receptor binding phenotypes (reviewed in (28)), and the PfEMP1 domains that bind to host endothelial
93 cell receptors such as CD36 (29), ICAM-1 (30) and endothelial cell protein receptor (EPCR) (31) are
94 well-characterised. However, current understanding of the molecular interactions that cause
95 rosetting is based on just eight PfEMP1 variants from six culture-adapted *P. falciparum* genotypes (14,
96 15) (17, 32). Seven of the eight characterised rosette-mediating PfEMP1 variants are encoded by
97 group A *var* genes, and have a DBLα1 domain of subclass 1.5, 1.6 or 1.8 (Figure 1A). These domains
98 are followed by a CIDRβ, γ or δ domain, completing DC11 in two of the characterised rosetting variants
99 (IT4VAR60 and TM284VAR1), DC16 in three variants (3D7PF13_000, HB3VAR06 and MUZ12 VAR1) and
100 DC16-like (similar to DC16, but with CIDRγ rather than CIDRδ) in two variants (IT4VAR09 and PAVARO)
101 (Figure 1B). These domain classes and cassettes therefore define a rosetting-associated head structure
102 (DBLα1.5/6/8-CIDRβ/γ/δ).

103 A single previously characterised candidate rosetting variant, TM180VAR1, is encoded by a
104 group B/A *var* gene that lacks the rosetting-associated head structure (17). This gene has a "DC8-like"
105 head structure, with a DBLα2 domain followed by a CIDRα1.8 domain (Figure 1A), whereas DC8 usually
106 has a CIDRα1.1 domain (Figure 1B) (27). The unusual architecture of this variant, along with the
107 observation that antibodies against the DBLα domain did not disrupt rosettes in this parasite line (17),

108 means that the evidence supporting this as a rosette-mediating PfEMP1 type is weaker than for the
109 other reported variants, and it remains possible that the TM180 parasite line forms rosettes via a
110 PfEMP1-independent mechanism.

111 Due to the small number of characterised rosetting PfEMP1 variants to date, we currently
112 lack a model to predict with confidence from parasite genomic sequence data which PfEMP1 variants
113 mediate rosetting and which do not. In this study, we hypothesized that the rosetting phenotype in
114 diverse *P. falciparum* isolates is encoded by either DC11 or DC16 PfEMP1 variants. We tested this
115 hypothesis by firstly identifying PfEMP1 variants with the predicted rosetting head structure in the
116 genomes of thirteen recently culture-adapted Kenyan *P. falciparum* lines, then selected four of these
117 lines for rosetting and characterised their *var* gene/PfEMP1 expression. We also examined whether
118 the DC8-like candidate rosetting variant TM180VAR1 has erythrocyte-binding function. Our findings
119 confirm the importance of DC11 and DC8-like variants in rosetting and identify another previously
120 unrecognised PfEMP1 domain cassette (DC15) that binds to uninfected erythrocytes to mediate
121 rosette formation.

122

123 **Results**

124 ***Selection of high rosetting (R+) Kenyan P. falciparum lines***

125 Thirteen culture-adapted *P. falciparum* lines, originally isolated from children with *P. falciparum*
126 malaria in Kenya, were studied (33, 34). The full *var* gene/PfEMP1 repertoire sequences of these
127 parasites were published previously (35), and are shown in diagrammatic form in Figure S1. On
128 examining the repertoires, the number of PfEMP1 variants with the predicted rosetting-associated
129 head structure (DBLα1.5/6/8-CIDR$\beta/\gamma/\delta$) ranged from 0 to 7 (median 3) per parasite line (Table 1). We
130 cultured each of the Kenyan *P. falciparum* lines for at least two replication cycles *in vitro* and screened
131 the mature-infected erythrocytes for spontaneous rosette formation by microscopy. Rosettes were
132 detected in four of the parasite lines, at a high level in KE10 (>50% of infected erythrocytes in rosettes)
133 and a low level in PC0053, KE11 and KE08 (2-10% of infected erythrocytes in rosettes). The absence of

134 rosetting in the other parasite lines, despite their genomes containing group A *var* genes encoding
135 PfEMP1 variants with the rosetting head structure, is not surprising because previous work has shown
136 that parasites tend to switch off group A *var* genes when adapted to culture (36). The four rosette-
137 positive lines were grown in continuous culture and selected using density gradient methods to
138 generate isogenic pairs of high rosetting (R+, >60% of infected erythrocytes in rosettes) and low
139 rosetting (R-, <2% of infected erythrocytes in rosettes) parasite lines for each genotype. Parasite line
140 KE11R+ was resistant to selection for a high rosette frequency using conventional methods, possibly
141 due to a high frequency of *var* gene switching. Therefore, further study of KE11R+ was carried at a
142 rosette frequency of ~15-30% of infected erythrocytes in rosettes.

143

144 **Table 1.** The Kenyan *P. falciparum* parasite lines screened for the formation of rosettes *in vitro*.

Parasite line[#]	**Pf3K designation[#]**	**Clinical syndrome***	**Group A *var* genes[$]**	**Predicted rosetting head structure[†]**	**Rosettes seen *in vitro***	**Human IgM-Fc binding[&]**
9106	PFKE01	IC	7	1	No	ND
9626	PFKE02	UM	15	3	No	ND
8383	PFKE03	UM	9	2	No	ND
10668	PFKE04	IC, RD	14	4	No	ND
11014	PFKE05	SMA	6	2	No	ND
10936	PFKE06	UM	11	6	No	ND
10975	PFKE07	SMA	23	7	No	ND
9605	**PFKE08**	**IC**	**8**	**4**	**Yes**	**No**
6816	PFKE09	IC	6	0	No	ND
11019	**PFKE10**	**IC**	**10**	**3**	**Yes**	**Yes**
9775	**PFKE11**	**UM**	**13**	**3**	**Yes**	**No**
9215	PFKE12	RD	12	3	No	ND
9197	**PC0053**	**IC**	**8**	**3**	**Yes**	**No**

145 [#]The name of each parasite line according to the KEMRI-Wellcome Trust Laboratory parasite naming
146 system (33, 34) and its designation in the Pf3k database (35) is given.

147 *The clinical syndrome of the patient from whom the parasite isolate was collected. IC, impaired
148 consciousness; UM, uncomplicated malaria: RD, respiratory distress; SMA, severe malarial anaemia.
149 [$]The total number of group A *var* genes in each parasite's genome.
150 [†]The number of *var* genes in each parasite's genome that encode the rosetting-associated head
151 structure DBLα1-CIDRβ/γ/δ.
152 [&]Determined by immunofluorescence assay/flow cytometry of live infected erythrocytes with an anti-
153 human IgM (μ chain) antibody. ND, not done.
154
155
156 ***IgM-binding and trypsin-sensitivity of rosetting in the Kenyan R+ parasite lines***

157 Previous work has shown that some *P. falciparum* rosetting lines bind the Fc region of human IgM,
158 and this promotes rosette formation, possibly by clustering PfEMP1 molecules to increase binding
159 avidity (37-39). The dual rosetting and IgM-Fc binding phenotype is strongly associated with severe
160 malaria (40, 41) and the known PfEMP1 variants that mediate this dual binding are mostly of the DC11
161 type (Figure 1) (17, 37, 38, 42). Due to the presence of human serum in the parasite culture medium,
162 IgM-binding can be detected by immunostaining of live infected erythrocytes taken directly from
163 culture. Hence, the four R+ lines were assessed for their IgM-binding ability by staining with anti-
164 human IgM antibodies. Infected erythrocytes of the KE10R+ parasite line were IgM positive, whereas
165 the other three R+ lines were IgM negative (Figure 2A, Table 1).

166 PfEMP1 is characteristically highly sensitive to trypsin digestion (17, 43), whereas RIFINs and
167 STEVORS, which have also been implicated in rosetting, are not (44, 45). Therefore, to determine
168 whether PfEMP1 was the likely rosette-mediating parasite adhesion molecule in the Kenyan rosetting
169 lines, infected erythrocytes were treated with a low dose of trypsin and rosette frequency was
170 assessed. Rosetting in all four lines was abolished by treatment with 1μg/ml trypsin for five minutes,
171 consistent with a PfEMP1-dependent rosetting mechanism (Figure 2B).

172

173 ***var gene profiling to identify predominant rosetting-associated PfEMP1 variants***

174 To identify the predominant *var* genes specifically transcribed in the R+ parasite lines, we carried out
175 DBLα tag profiling of the R+/R- isogenic pairs (14, 46). The full *var* gene sequence for each
176 predominant tag was retrieved from the Pf3k database (35) or determined by extension PCR and

177 sequencing. For clarity, the predominant rosette-specific *var* gene identified in each parasite line is
178 referred to here as '*parasite line name var_r1'* with the full name of each gene from the Pf3K database
179 also given on first use. *var* gene profiling of KE10R+ and KE10R- parasite lines showed that the
180 *pfke10var_r1* (*PX0203.g54)* gene encoding a DC11 PfEMP1 variant was the predominant transcript
181 expressed only in the rosetting line (Figure 3 and Figure 4). Parasite lines PC0053R+ and KE11R+ both
182 expressed two predominant transcripts. However, in each case, only one was exclusively expressed
183 by the R+ line (Figure 3). Therefore, *pc0053var_r1 (PC0053-C.g687)* and *pfke11var_r1 (PFKE11.g448),*
184 encoding PfEMP1 variants containing DC15 (DBLα1.2-CIDRα1.5b), were identified as the candidate
185 rosette-mediating adhesins (Figure 4). This head structure has not previously been associated with
186 rosetting. *var* gene profiling of the KE08R+ and KE08R- parasite lines identified two predominant
187 transcripts in the R+ population, *pfke08var_r1 (PFKE08.g502)* and *pfke08var_r2 (PFKE08.g501)* (Figure
188 3). Expression of *pfke08var_r2* was not detected in the R- population, whereas *pfke08var_r1* was
189 detected at a low level (5% of transcripts). *pfke08var_r1* encodes a DC11 rosetting-associated head
190 structure, whereas *pfke08var_r2* is a group B/A *var* gene, encoding DC8 (DBLα2-CIDRα1.1) (Figure 4).
191 DC8 PfEMP1 variants are usually associated with binding to human brain endothelial cells via EPCR
192 (47), and not with rosetting, with the exception of the unusual putative rosetting variant TM180VAR1*,*
193 which has a "DC8-like" architecture (17). Therefore, in this case, both *pfke08var_r1* and *pfke08var_r2*
194 were considered to be potential rosette-mediating PfEMP1 variants and were investigated further.
195
196 ***Staining of infected erythrocytes for surface expression of candidate rosetting-associated variants***
197 We next raised antibodies to the candidate rosetting PfEMP1 variants identified above, to determine
198 whether the specific PfEMP1 variants were present on the surface of live infected erythrocytes. The
199 NTS-DBLα region of each variant was expressed as a recombinant protein in *E. coli* (Figure S2) and
200 used to immunise rabbits to generate polyclonal antibodies against PfEMP1 as described previously
201 (17, 48). The antibodies were used in indirect immunofluorescence and flow cytometry with live
202 infected erythrocytes. Non-immunised rabbit IgG or IgG raised to an irrelevant PfEMP1 NTS-DBLα

203 protein (HB3VAR03, which binds to human brain endothelial cells (49)) were used as negative controls,
204 and the gating strategy to identify the mature pigmented-trophozoite and schizont stage infected
205 erythrocyte population which displays PfEMP1 as a DNA/RNA high population is shown in Figure S3.
206 In each case, the IgG against the candidate rosetting PfEMP1 variant stained live rosetting
207 infected erythrocytes of the respective parasite line at a frequency comparable to the rosette
208 frequency, whereas the isogenic R- lines were negative (Figure 5). Unexpectedly, in the KE08R+ line
209 ~90% of mature infected erythrocytes stained positively with both the KE08VAR_R1-specific rabbit IgG
210 and the KE08VAR_R2-specific IgG (Figure 5E and G). This suggests either antibody cross-reactivity or
211 the possibility that both PfEMP1 variants are expressed on the same infected erythrocytes. Usually
212 only one PfEMP1 type is expressed per infected erythrocyte, due to mutually exclusive expression of
213 *var* genes (50). However, one previous example of a parasite line simultaneously expressing two
214 different PfEMP1 variants on the same infected erythrocyte has been described (51). To examine
215 KE08R+ in more detail, we raised antibodies against the N-terminal CIDR domains of the two
216 predominantly expressed PfEMP1 types and repeated the immunofluorescence staining. Once again,
217 the polyclonal rabbit IgG raised against the KE08VAR_R1 CIDR domain and the KE08VAR_R2 CIDR
218 domain both stained a similar major population of infected erythrocytes in the rosetting line,
219 consistent with expression of both variants on the surface of infected erythrocytes (Figure 5I and K).
220
221 ***Rosette disrupting activity of anti-PfEMP1 IgG***
222 Next, we assessed the ability of the rabbit IgG raised against the candidate rosetting variants to disrupt
223 rosettes in their respective lines. IgG from antisera raised to the NTS-DBLα domain of an irrelevant
224 PfEMP1 variant (HB3VAR03) and IgG purified from the sera of a non-immunised rabbit were used as
225 negative controls. The KE11R+ line was not included in these assays, due to the difficulty in
226 maintaining a sufficiently high level of rosetting. For parasite lines KE10R+ and PC0053R+, rosetting
227 was completely abolished by 10μg/ml of rabbit IgG to the relevant PfEMP1 NTS-DBLα domain (Figure
228 6A and B), supporting the identification of KE10VAR_R1 (DC11) and PC0053VAR_R1 (DC15) as rosette-

229 mediating PfEMP1 types. In the KE08R+ line, rosettes were abolished by 10μg/ml of IgG to the NTS-
230 DBLα domain of KE08VAR_R1 (DC11), but there was no effect on rosetting of IgG to KE08VAR_R2
231 (DC8) (Figure 6C), despite these antibodies recognising the surface of KE08R+ infected erythrocytes
232 (Figure 5G). This suggests that it is the DC11 variant KE08VAR_R1 and not the DC8 variant KE08VAR_R2
233 that is the rosette-mediating adhesion molecule in the KE08R+ parasite line.
234
235 ***Functional assays to detect PfEMP1 binding to uninfected erythrocytes and IgM***
236 Previous studies have identified the NTS-DBLα domain as the erythrocyte-binding region of rosette-
237 mediating PfEMP1 variants (14, 15, 17, 32). To examine the erythrocyte binding function of the
238 candidate rosetting variants, NTS-DBLα and CIDR recombinant proteins were incubated with
239 uninfected erythrocytes and bound protein detected by flow cytometry. The NTS-DBLα domain of the
240 well-characterised rosetting variant IT4var60 (15, 17) was included as a positive control, alongside
241 negative controls which were NTS-DBLα domains from human brain endothelial cell binding PfEMP1
242 variants that are expressed by parasite lines that are known to be non-rosetting (49).
243 The NTS-DBLα domains of the candidate rosetting variants KE10VAR_R1 (DC11),
244 PC0053VAR_R1 (DC15), KE11VAR_R1 (DC15) and KE08VAR_R1 (DC11) all bound to uninfected
245 erythrocytes, confirming their identification as rosette-mediating variants (Figure 7A-F). Neither the
246 NTS-DBLα or CIDR domain from KE08VAR_R2 bound to erythrocytes, consistent with the above
247 suggestion that KE08VAR_R2 is not a rosette-mediating variant (Figure 7A and G). The CIDR domains
248 of KE08VAR_R1 and KE11VAR_R1 also did not bind to erythrocytes, consistent with previous data
249 showing NTS-DBLα to be the major erythrocyte-binding domain of rosette-mediating PfEMP1 variants
250 (Figure 7A) (14, 32, 52).
251 For the IgM Fc-binding rosetting line KE10R+, the domains downstream of the head structure
252 were expressed as recombinant proteins and tested for human IgM binding by ELISA. Previous work
253 has identified either the ultimate DBLε or penultimate DBLζ domain as the IgM-binding region of

254 PfEMP1 (Figure 1) (37-39, 53). Consistent with this, DBLζ3 was identified as the IgM-binding domain
255 of KE10VAR_R1 (Figure 8).
256
257 ***The "DC8-like" variant TM180VAR1 mediates rosetting***
258 The rosetting line TM180R+ expresses the group B/A *var* gene *tm180var1*, which lacks the rosetting
259 associated head structure (Figure 1) (17). To test the hypothesis that TM180R+ forms rosettes via a
260 variant surface antigen other than PfEMP1, TM180R+ was treated with low-dose trypsin as described
261 above. TM180R+ rosetting was abolished by 5 μg/ml of trypsin, suggestive of a PfEMP1-mediated
262 rosetting mechanism rather than an alternative RIFIN- or STEVOR-mediated mechanism (Figure 9A).
263 The TM180VAR1 NTS-DBLα recombinant protein was tested in the erythrocyte binding flow cytometry
264 assay, and showed unequivocal binding to uninfected erythrocytes, confirming its role in rosetting
265 (Figure 9B).
266
267 ***KE08R+ binds to ICAM-1 and EPCR as well as forming rosettes***
268 The simultaneous expression and surface display of KE08VAR_R1 and KE08VAR_R2 shown above raise
269 the possibility that the KE08R+ parasite line might have an unusual adhesion phenotype. KE08VAR_R2
270 contains CIDRα1.1 and DBLβ12 domains, that characteristically bind EPCR and ICAM-1, respectively
271 (30, 47). Static binding experiments showed that KE08R+ infected erythrocytes bound to EPCR and
272 ICAM-1 (Figure 10). Notably, significantly higher binding was seen when rosettes were disrupted with
273 rabbit IgG to KE08VAR_R1 prior to the binding assay, suggesting that once rosettes have formed, they
274 impede binding to other receptors in adhesion assays, as shown previously (54). This suggests that, by
275 expressing two *var* genes simultaneously, KE08R+ infected erythrocytes exhibit an unusual "triple"
276 virulence-associated adhesion phenotype - rosetting, ICAM-1 binding and EPCR-binding.
277
278 ***Presence of rosetting-associated motifs and binding sites in the novel rosetting PfEMP1 variants***

279 Having identified four new rosette-mediating PfEMP1 variants, we examined a multiple sequence
280 alignment of known rosetting and non-rosetting NTS-DBLα amino acid sequences to determine if
281 previous motifs (4) and homology blocks (HB) (55) associated with high rosetting are found in the new
282 variants and are conserved across all rosetting variants. The motif "MFKPNKDKVEG" that contains
283 HB219 (55) and the adjacent high rosetting "H3" motif (4) was seen in all of the newly described
284 variants and this sequence is over-represented in rosetting compared to non-rosetting variants (green
285 box, Figure 11). The other Normak et al (4) high rosetting motifs (H1 and H2) were not found. Two
286 other motifs in the central region of NTS-DBLα "YKDGSG" (red box, Figure 11) and "TCKAPQDAN" (blue
287 box, Figure 11) were found in the newly identified variants and are strongly over-represented in the
288 rosetting variants overall.
289
290 **Discussion**
291 Here we have identified four novel rosette-mediating PfEMP1 variants, determined by *var* gene
292 profiling, infected erythrocyte surface expression of PfEMP1, rosette disruption with antibodies to
293 PfEMP1 and functional studies showing NTS-DBLα binding to uninfected erythrocytes. Two of the
294 variants identified, KE10VAR_R1 and KE08VAR_R1 contain DC11, giving them comparable PfEMP1
295 architecture to the previously described rosetting variants TM284VAR1 and IT4VAR60 (Figure 1) (15,
296 17, 37). The other two new rosetting variants, PC0053VAR_R1 and KE11VAR_R1, have a DC15 head
297 structure, not previously implicated in rosetting. Instead, DC15 PfEMP1 variants were thought to bind
298 EPCR via their CIDRα1.5 domain (31). However, CIDRα1.5 domains fall into two clear subtypes,
299 CIDRα1.5a and CIDRα1.5b (31). The DC15 variants identified here have an NTS-DBLα1.2 domain that
300 binds to erythrocytes (Figure 7), followed by CIDRα1.5b, a domain type which when investigated
301 previously only bound weakly to EPCR (31). Thus, rosetting DC15 variants may represent a functionally
302 distinct group, possibly characterised by the presence of CIDRα1.5b (Figure S4), although further work
303 is needed confirm this. Our study also showed that the NTS-DBLα2 domain of a "DC8-like" variant

304 encoded by *tm180var1* binds to uninfected erythrocytes, confirming this as a rosette-mediating
305 variant (17).

306 These findings combined with previous work show that at least four different group A and B/A
307 PfEMP1 types mediate rosetting: DC11, DC16, DC15 (with CIDRα1.5b) and DC8-like, with only the first
308 two containing the recognised rosetting-associated head structure of DBLα1.5/6/8-CIDRβ/γ/δ. It
309 remains unknown whether these different rosette-mediating PfEMP1 types have functional
310 significance, for example, binding to different host receptors on uninfected erythrocytes (56), and this
311 should be explored in future. Recent work also suggests that a group C PfEMP1 variant
312 PF3D7_0412900 can mediate rosetting by binding to Glycophorin B on uninfected erythrocytes (57).
313 Taken together, these data show that a more diverse set of PfEMP1 types mediates rosetting than
314 originally recognised. Further investigation will be needed to determine whether all PfEMP1 variants
315 containing these particular rosetting-associated DCs mediate rosetting. Our analysis of the *var* gene
316 repertoires of the thirteen Kenyan parasite lines showed that on average, there are three *var* genes
317 per *P. falciparum* genome encoding a DC11 and/or DC16 variant (Table 1). Many of these parasite
318 lines also have one or more *var* gene encoding a DC15 (CIDRα1.5b) and/or a DC8-like variant
319 containing a CIDRα1.8 domain rather than the CIDRα1.1 found in classical non-rosetting EPCR-binding
320 DC8 variants (31). If the DC types identified here always mediate rosetting, this would imply that about
321 one third of the group A and B/A *var* genes per *P. falciparum* isolate encode rosetting variants,
322 consistent with an important biological role for this phenotype. Exactly how rosetting benefits the
323 parasite is unclear, but an *in vivo* model showed that rosetting parasites reach a high parasite burden
324 more rapidly than isogenic non-rosetting parasite (58), which could increase parasite fitness by
325 enhancing transmission (59). More rapid expansion *in vivo* could be due to rosetting enhancing
326 erythrocyte invasion or reducing immune-mediated clearance, with current experimental evidence
327 favouring the latter hypothesis (60-62).

328 Previous work has demonstrated a strong association between rosetting and severe malaria
329 (2-5), with human IgM-binding rosetting isolates being particularly common in parasites collected

330 from African children with severe malaria (40, 41). Whether all rosetting phenotypes mediated by the
331 different DC types shown here have associations with severe malaria is unknown. Analyses of parasite
332 *var* gene transcription and clinical malaria severity have repeatedly shown that expression of group A
333 *var* genes and those encoding DC8 are associated with severe disease (21-25). As shown here and
334 previously (17, 37), the IgM-binding rosetting phenotype is mediated by DC11 or DC16 PfEMP1
335 variants, and a recent study found expression of DC11 was associated with severe malaria in
336 Mozambiquan children (63), while both DC16 and DC15 were associated with severe malaria in
337 malaria-naïve adults (64). Many prior studies on *var* gene transcription and malaria severity do not
338 include primer sets for DC11 (22, 24, 25), raising the possibility that the contribution of this IgM-
339 binding rosette-mediating variant type to severe malaria could be greater than currently appreciated.
340 Understanding how *var* gene transcription relates to parasite adhesion phenotype is important in
341 facilitating the interpretation of *var* gene profiling/disease severity studies and can help identify the
342 key adhesion phenotypes that should be targeted therapeutically to treat or prevent severe disease.
343 One of the most underexplored topics in rosetting research is understanding how rosettes
344 sequester *in vivo*. Rosettes do not circulate in the peripheral blood and "rosette-like" aggregates of
345 infected and uninfected cells can be seen in the microvasculature in autopsy studies of cerebral
346 malaria patients (65-67). Sequestration of rosetting infected erythrocytes may require a dual binding
347 phenotype with simultaneous binding to receptor(s) on vascular endothelium as well as on
348 erythrocytes (68, 69). However, host endothelial cell receptors for rosetting PfEMP1 variants remain
349 poorly characterised. One in vitro study found that the rosetting line IT4VAR09/R29R+, which
350 expresses a DC16-like variant (Figure 1), adhered to a human brain endothelial cell line via the DBLγ15
351 domain, which interacted with an unidentified host heparan sulfate proteoglycan (69). It is notable
352 that all of the experimentally-proven rosetting variants, including the four new ones described here,
353 contain DBLγ as the third or fourth extracellular domain from the N-terminus, and we hypothesize
354 that binding of DBLγ to endothelial cell heparan sulfate is a common mode of sequestration for

355 rosetting infected erythrocytes. It is plausible that the diverse CIDRβ/γ/δ/α1 domains of rosetting
356 variants may alos bind to additional host receptors, and this remains to be explored.

357 Another feature of some rosette-mediating variants is the ability to bind serum proteins such
358 the human IgM-Fc and α2M, a phenomenon that clusters PfEMP1 to increase binding avidity (37, 38)
359 (39, 42). The IgM-Fc binding rosetting variants identified to date all contain a C-terminal triplet of DBLε
360 and DBLζ domains (17), but only one of these domains in each variant binds IgM (37-39, 53). We show
361 here that KE10R+ infected erythrocytes bind IgM via the DBLζ3 domain of KE10VAR_R1, consistent
362 with previous data. Interestingly, the KE08R+ and PC0053R+ parasite lines did not bind IgM, despite
363 their PfEMP1 variants containing a C-terminal DBLε/ζ domain triplet (Figure 4). Therefore, the
364 presence of a C-terminal DBLε/ζ domain triplet is not always predictive of IgM binding in rosetting
365 variants, although in the case of KE08R+, the expression of two different PfEMP1 variants at the
366 surface of infected erythrocytes might interfere with binding function at the membrane-proximal part
367 of PfEMP1.

368 The majority of evidence to date suggests that expression of PfEMP1 is mono-allelic (50, 70).
369 However, here we clearly demonstrate the simultaneous expression of two different group A PfEMP1
370 variants on the surface of infected erythrocytes of parasite line KE08R+, one mediating rosetting and
371 the other binding to EPCR and ICAM-1. A similar finding was reported previously, with a *P. falciparum*
372 3D7 parasite line expressing two PfEMP1 variants PFD1235w and PF11_0008, conferring a dual
373 binding phenotype to PECAM-1 and ICAM-1, which increased binding efficiency to endothelial cells
374 (51). Dual binding phenotypes are more commonly described in the context of single PfEMP1 variants,
375 with different domains within the same molecule binding different receptors (30, 69). It seems likely
376 that the ability to adhere to multiple receptors is advantageous to the parasite by strengthening
377 adhesion and thereby promoting sequestration. The multiple adhesion phenotypes seen in both
378 KE08R+ and the 3D7 line described above could be artefactual, for example with loss of mono-allelic
379 *var* gene transcription due to mutations introduced by the culture adaptation process. Or they could
380 represent genuine aspects of parasite biology that remain to be explored. Existing bulk RNA *var* gene

381 profiling studies in clinical isolates would not detect polygenic *var* gene transcription, and single cell
382 studies of clinical isolates will be needed to determine whether multiple *var* genes are transcribed per
383 infected erythrocyte in natural infections.

384 The increasing availability of *var* gene sequence data has revolutionised the ability to study
385 PfEMP1 diversity across multiple *P. falciparum* isolates (35). However, making functional sense of
386 these data relies on the ability to infer binding phenotype from *var* gene sequence. Excellent progress
387 has been made with PfEMP1 variants that bind to CD36, ICAM-1 and EPCR (29-31), and the work
388 described here is a step towards a more comprehensive understanding of rosette-mediating PfEMP1
389 variants. Important unanswered questions for future work include how many different PfEMP1 types
390 mediate rosetting, which host receptor(s) are they binding and are they suitable targets for
391 interventions such as strain-transcending antibodies to treat or prevent severe malaria (17, 71)?
392

393 **Materials and Methods**

394 ***Parasite culture and rosette selection***

395 The Kenyan parasite lines (Table 1) were collected from children with severe or uncomplicated *P.*
396 *falciparum* malaria between 2009 and 2010 in Kilifi, Kenya and were adapted to culture at the
397 Wellcome-Kenya Medical Research Institute (KEMRI) laboratories (33). The parasite lines are available
398 from the European Malaria Reagent Repository (http://www.malariaresearch.eu/). Parasites were
399 thawed and cultured in complete RPMI with 5% pooled human serum and 0.25% albumax and human
400 blood group O erythrocytes as described (71). Isogenic pairs of high and low rosetting cultures were
401 selected using density gradient methods (72).

402 ***Analysis of the var gene repertoires of the Kenyan parasite lines***

403 The PfEMP1 domain boundaries and architecture for the Kenyan parasite lines were obtained from a
404 previous study (35). The PfEMP1 repertoire for each parasite line was plotted using R v4.2.2 (73) and
405 arranged based on the 5' ups group of each protein (A, B then C). The domains were colour-coded as

406 previously described (27). The PFKE10VAR1 domain architecture was generated as described in the
407 *pfke10var1* sequence extension section below.

408 ***Assessment of rosette frequency***

409 Rosette frequency was assessed by staining an aliquot of culture suspension at ~2% haematocrit with
410 ethidium bromide (final concentration 25 μg/ml) and examination of a wet preparation using
411 simultaneous fluorescence/bright field microscopy on a Leica DM 2000 fluorescent microscope with
412 a x40 objective. A rosette was defined as an infected erythrocyte binding at least two uninfected
413 erythrocytes, and the rosette frequency expressed as the proportion of infected erythrocytes forming
414 rosettes out of 200 infected erythrocytes counted.

415 ***IgM-binding - immunofluorescence and flow cytometry***

416 Staining for human IgM was performed by incubating aliquots of live parasite culture in PBS/1%BSA
417 with 20μg/ml rabbit IgG against PfEMP1 NTS-DBLα for 45 mins then washing three times with PBS.
418 The washed cells were incubated in PBS/1% BSA containing 1/2500 of Vybrant™ DyeCycle™ stain with
419 1/1000 Alexa Fluor™ 647-conjugated cross-absorbed goat anti-rabbit IgG (Invitrogen, A-21244) and
420 1/1000 Alexa Fluor™ 488-conjugated cross-adsorbed goat anti-human IgM (heavy chain specific)
421 (Invitrogen, A-21215) before washing as above and fixing in PBS/0.5% paraformaldehyde. The samples
422 were used to make thin smears for microscopy or read on a BD LSRFortessa instrument (BD
423 Biosciences) with data from least 500 mature parasitised erythrocytes collected per sample. Data were
424 analysed in FlowJo v.10 and the gating strategy is shown in Figure 2A. As a negative control, parasites
425 were grown as described above in complete RPMI but with 5% IgM-deficient human serum, prepared
426 by five consecutive 30 minute rounds of incubation with anti-human IgM beads (Sigma-Aldrich
427 A9935).

428 ***Trypsinisation of parasitised erythrocytes***

429 Mature pigmented trophozoites were purified from 100µl packed cell volume of parasite culture at
430 >4% parasitaemia using magnetic purification as described (71). The purified parasites were washed
431 twice before being resuspended in 100µl of trypsin (Sigma-Aldrich T4799) in PBS at concentrations 0,

432 0.5, 1 and 5µg/ml, and incubated at 37°C for 5 mins. Cells were pelleted by centrifugation and the
433 pellet resuspended in 1 mg/ml soybean trypsin inhibitor (Sigma-Aldrich T9003) and incubated at 37°C
434 for 5 mins. The cell pellet was washed and resuspended in complete binding media (RPMI 1640
435 without bicarbonate with 25 mM HEPES, 16mM glucose, 25µg/ml gentamicin, and 10% human
436 serum). O+ blood was added to each sample to a final parasitaemia of 20%, mixed, and incubated at
437 37°C for 1 hour. The cells were then pelleted before being resuspended by gentle pipetting and rosette
438 frequency assessed. Samples were assayed in duplicate and the mean of the two rosette frequency
439 counts taken.

440 ***DBLα sequence tag RT-PCR***

441 RNA was extracted from parasite cultures when they at the mid-late ring/very early trophozoite stage
442 (~10-20 hours post invasion) by resuspending pelleted cells in 10x volumes of Trizol (Ambion
443 15596026). RNA was extracted, cleaned and concentrated using bromochloropropane (Sigma-Aldrich
444 B9673) and a Zymo Research RNA Clean & Concentrator Kit (R1014) according to the manufacturer's
445 instructions for Trizol clean-up with minor modifications. Samples were treated with the TURBO
446 DNase-Free Kit (Invitrogen AM1907) before cDNA was made from 8µl RNA using the SuperScript ® III
447 First-Strand Synthesis System for RT-PCR (Invitrogen 18080-051) with random hexamers. DBLα-tag 50
448 µl PCR reactions contained 2µl of cDNA, 20.75 µl of dH_2O, 4 µl of 25mM $MgCl_2$, 8 µl of 1.25mM dNTPs
449 (Promega U120A, U121A, U122A, U123A), 5 µl of αAF2 primer (GCACG(A/ C)AGTTT(C*/T)GC) (46), 5
450 µl of αBR primer (GCCCATTC(G/C)TCGAACCA) (46), and 5 µl of Amplitaq Gold buffer with 0.25 µl
451 Amplitaq Gold (1.25 units) (Applied Biosystems 4311816). The reactions were cycled as follows,
452 95°C for 5 mins, 95°C for 20 s, 42°C for 20 s, 60°C for 1 minute, 60°C for 10 mins, 4°C to hold.
453 The PCR products were cleaned using a Nucleospin Gel and PCR Clean-up kit (Macherey-Nagel
454 740609.250) then cloned into the pCRII vector using a TA Cloning Kit Dual Promoter pCRII Vector
455 (Invitrogen K207020) at a vector to insert ration of 1:3. TOP10F' One Shot Competent Cells (Invitrogen
456 440300) were transformed using 2µl of each ligation reaction. 24 colonies were picked per ligation
457 and grown overnight before plasmids were isolated from the cultures using a GeneJET Plasmid

458 Miniprep Kit (ThermoFisher Scientific K0502). Plasmid inserts were Sanger sequenced at the MRC
459 Protein Phosphorylation and Ubiquitiylation Unit, Dundee (https://dnaseq.co.uk/) using the forward
460 primer VF1 (AGCTCGGATCCACTAGTA) and the resulting amino-acid sequences were used in a BLAST
461 search (74) against the *var* gene/PfEMP1 repertoire of the relevant *P. falciparum* line to identify the
462 full-length gene sequence.

463 **pfke10var1 sequence extension**

464 For completion of the *pfke10var1* Exon 1 sequence (which was incomplete in the database), a forward
465 primer (11019F2 5' GATTTTGACACATC CAAAGTGT) was designed targeting the *pfke10var1* DBLZ3
466 domain at approximately 200bp from the end of the partial sequence. This was paired with a reverse
467 primer (Exon2_3.3 5' CCATTTCTTCATATTCACTTTC) targeting a conserved region in Exon 2 (75).
468 50pmols of each primer was added to a reaction mix containing 1.25mM dNTPs, 1.5mM $MgCl_2$, 1x
469 Platinum *Pfx* buffer (Invitrogen 11708), 1 unit of Platinum *Pfx* DNA polymerase (Invitrogen 11708),
470 0.2µg cDNA and made up to a final reaction volume of 50µl. The PCR conditions were initial
471 denaturation at 95°C for 5 mins followed by 35 cycles of denaturation at 95°C for 5 secs, annealing at
472 52°C for 15 secs and extension at 60°C for 3 mins. A final extension was performed at 60°C for 10
473 minutes and the amplicon was resolved in a 1% agarose gel at 70V for 50 minutes to reveal a 2kb
474 band. This was then gel purified using a purification kit (Macherey-Nagel 740609) following the
475 manufacturer's instructions. The purified PCR product was Sanger sequenced using both the forward
476 and reverse sequences listed above. From the newly generated sequence from the forward primer,
477 another primer sequence was designed (11019P1 5' GAGTGTAAAGTTGAGTCCCTTG) targeting a region
478 approximately 400bp downstream which was then used to further sequence the original 2kb PCR
479 product. The Sanger sequencing results from the three primers (11019F2, 11019P1 and Exon 2) and
480 the partial Exon 1 sequence were then aligned to generate the complete Exon 1 sequence. To define
481 the domain boundaries of the complete KE10VAR_R1 Exon 1 protein sequence, the sequence was
482 submitted to VarDom (https://services.healthtech.dtu.dk/services/VarDom-1.0/)(27) for annotation.

483 The subclasses were resolved by using the individual domains in a BLAST search (74) against the Pf3k
484 database (35) and identifying the subclass of the top hit based on full length alignment.

485 ***Recombinant protein production***

486 Codon optimised sequences for *E. coli* expression of PfEMP1 domains with a BamHI site at the 5' end
487 and an NheI site at the 3' end were obtained from Twist Biosciences (San Francisco, California) and
488 ligated into the expression vector modified pET15b (pET15b conv) (76). The DBLα domain sequences
489 included the N-terminal sequence. All proteins were synthesised with a His-tag at the N-terminal end
490 of the sequence. Ligation reactions were sequenced to confirm the correct insert sequence. Origami
491 B cells containing pRIG were transformed using the recombinant plasmids (76). Protein expression
492 was induced by the addition of IPTG and the bacteria harvested. Cell pellets were frozen before
493 resuspension in Bugbuster mastermix (Novagen 71456) and EDTA-free protease inhibitor tablets
494 (Roche 11836170001). Nickle-NTA or cobalt-NTA chromatography was used to purify the polyhistidine
495 (His)-tagged proteins. DBLα proteins were further purified by size exclusion chromatography as
496 described (17). For proteins KE10VAR_R1 DBLα, TM180VAR1 DBLα and PC0053VAR_R1DBLα the his-
497 tag was cleaved with TEV protease before use in experiments as described (17, 48). Fractions
498 containing protein were pooled and buffer exchanged into PBS using PD-10 desalting columns (Sigma-
499 Aldrich GE17-0851-01). The proteins were concentrated using Vivaspin 20ml 10 kDa or 30 KDa MWCO
500 concentrators (Merck Z614602-12EA) and stored in aliquots at -70 ^{o}C.

501 ***Rabbit immunisations and IgG purification from antisera***

502 Rabbit immunisations were done by BioGenes GmBH (Berlin, Germany). Preimmune sera were
503 screened to identify rabbits that did not have anti-human erythrocyte antibodies by
504 immunofluorescence assay as described (17, 48). Selected rabbits were immunised with 250μg of
505 antigen in BioGenes proprietary adjuvant (92.8% mineral oil, 3.48% Tween-20, 3.48% Span-80 and
506 0.23% lipopolysaccharides from *Phormidium spp*) on day 1 followed by boosting with 100μg of antigen
507 on days 7, 14, 28, 49 with the final bleed on day 56. Total IgG was purified from the resulting antisera

508 using a Pierce protein A IgG purification kit (ThermoFisher Scientific 44667) according to the
509 manufacturer's instructions.

510 ***Flow cytometry with PfEMP1 antibodies***

511 Staining of mature parasitised erythrocytes for PfEMP1 with rabbit IgG was done as described (71).
512 Briefly, whole culture was incubated for 45 minutes with rabbit IgG against the relevant PfEMP1
513 domain at a final concentration of 20μg/ml before being washed three times with PBS. The cells were
514 then incubated in PBS/1% BSA containing 1/2500 of VybrantTM DyeCycle™ stain with 20μg/ml
515 ethidium bromide and 1/1000 Alexa Fluor 647-conjugated cross-adsorbed goat anti-rabbit IgG
516 (Invitrogen A-21244) for 30 minutes. Cells were washed twice in PBS and once in PBS 1% BSA before
517 being fixed in PBS/0.5% paraformaldehyde. The samples were read on a BD LSRFortessa instrument
518 (BD Biosciences) in duplicate with at data from least 500 mature parasitised erythrocytes collected
519 per sample. Data were analysed with FlowJo v.10.

520 ***Rosette disruption assays***

521 Parasite culture at ~2% haematocrit was stained with ethidium bromide at a final concentration of
522 25μg/ml for 2 mins at 37°C. The cells were pelleted by centrifugation, the supernatant removed, and
523 the pellet resuspend at 2% haematocrit in complete binding medium as described above. 2.5μl of the
524 relevant anti-PfEMP1 rabbit IgG at 100, 10 or 1μg/ml was added to 22.5μl aliquots of stained culture
525 to give final concentrations of 10, 1 and 0.1μg/ml. An equivalent volume of PBS was added to the no
526 antibody control. The samples were incubated at 37°C for 1 hour in the dark with gentle resuspension
527 of cells every 10 mins before assessment of rosette frequency. Statistical analyses and graphs were
528 done using GraphPad Prism (Version 10.2.2, GraphPad software, Inc).

529 ***Erythrocyte binding assays***

530 The assay investigating the ability of recombinant PfEMP1 domains to bind to uninfected erythrocytes
531 was based on those described previously (52, 77). 10 μl of washed O+ erythrocytes were re-suspended
532 in 1ml PBS/1% BSA with 100μg/ml of recombinant protein and incubated on ice for 1 hour then
533 washed twice with 200 μl ice-cold PBS and resuspended in 23.75 μl of PBS/1% BSA. 1.25 μl of the

534 relevant rabbit IgG to the recombinant protein PfEMP1 domain at 1 mg/ml (final concentration 50
535 μg/ml) was added and incubated on ice for 45 mins before washing twice with 500μl PBS. The washed
536 cell pellets were resuspended in 50μl of PBS/1%BSA containing 1:1000 dilution of Alexa Fluor™ 488
537 goat anti-rabbit IgG (Invitrogen A-11034) and incubated for a further 45 mins on ice in the dark before
538 being washed twice. The cells were resuspended in 200μl of PBS containing 0.1% BSA and 0.01%
539 sodium azide and transferred to a 96 well plate. The 96 well plates were read on a BD LSRFortessa
540 instrument (BD Biosciences). Data were analysed in FlowJo v.10. For statistical analysis, median
541 fluorescence intensity (MFI) values were log transformed and analysed by one way ANOVA in
542 GraphPad Prism v10.

543 ***IgM Enzyme Linked Immunosorbent Assay (ELISA)***

544 An ELISA was used to test the interaction between IgM and KE10VAR_R1 domains as previously
545 described (37), with modifications. ELISA plates (Greiner 655061) were coated with 200 µl of 10 µg/ml
546 human IgM (Sigma 18260) diluted in 0.1 M carbonate-bicarbonate buffer and incubated at 4°C
547 overnight. Control wells contained buffer but no IgM. After incubation, the coating buffer was flicked
548 off and blocking buffer (PBS/5% skimmed milk/0.1% (v/v) Tween 20) was added for 2 hours at RT. The
549 plate was washed three times with PBS. KE10VAR_R1 DBL proteins were suspended in dilution buffer
550 (PBS/1% skimmed milk/0.1% (v/v) Tween 20) and 150 µl of each DBL protein at four 5-fold dilutions
551 (50 µg/ml, 10 µg/ml, 2 µg/ml, 0.4 µg/ml) were added to duplicate wells and incubated overnight at
552 4°C. After incubation, the plate was washed three times with PBS. 50 µl of anti-His HRP (1:3000)
553 (Biolegend 652404) in dilution buffer was added to each well and incubated at 37°C for 1 hour. The
554 plate was washed three times with PBS and twice with deionised water. 50 µl of 3,3',5,5'-
555 Tetramethylbenzidine (TMB) (Sigma, T2885) substrate was added to each well and incubated at RT for
556 7 mins. The reaction was stopped using 0.18 M sulphuric acid and absorbance read at 450nm. The
557 mean absorbance readings from duplicate wells were plotted against DBL protein concentration using
558 R v4.2.2 (73).

559 ***Host receptor spot binding assays***

560 3 μl spots of recombinant ICAM-1 (50 μg/ml; R&D 720-IC), EPCR (50 μg/ml; Sino Biologicals
561 13320-H02H), CD36 (25 μg/ml; R&D 1955-CD) and PBS, all in duplicate were spotted onto 60 mm
562 diameter bacteriological petri dishes (BD Falcon 351005) and incubated in a humidified chamber
563 overnight at 4°C. Next day the spots were aspirated and 2 ml of PBS/2% BSA blocking buffer was added
564 per dish and incubated for 2 hours at 37°C. During the blocking step, 1.5 ml aliquots of KE08R+ culture
565 suspension at 5-10% parasitemia (predominantly mature pigmented trophozoite stage) and ~2% Ht
566 were prepared by pre-incubation with or without 10 μg/ml of rabbit polyclonal IgG to KE08VAR_R1
567 NTS-DBLα for 30 mins at 37°C to disrupt rosettes. The blocking solution was removed, dishes washed
568 with incomplete binding medium (IBM, as described above but without serum) and 1.5 ml of the
569 prepared culture suspension was added to each dish. Dishes were incubated at 37°C for 1 hour, with
570 gentle resuspension every 12 minutes. Unbound cells were removed by at least five gentle washes
571 with 4 ml of IBM per wash; bound cells were fixed with PBS/2% glutaraldehyde for at least 30 mins
572 and stained with 5% Giemsa for 10 mins. The number of infected erythrocytes bound to each spot was
573 counted with an inverted microscope using a 40X objective. Technical replicates based on counts of
574 duplicate spots or dishes were averaged to determine a binding value for each receptor in each
575 experiment, and statistical analysis was done on the average binding values from $n \geq 3$ independent
576 experiments using one-way ANOVA with Dunnett's multiple comparisons test or two-tailed paired t
577 tests with Holm-Sidak multiple comparisons test. Statistical analyses and graphs were done using
578 GraphPad Prism (Version 10.2.2, GraphPad software, Inc).

579 ***Multiple sequence alignment and motif search***

580 Multiple sequence alignment (MSA) of the NTS-DBLα protein sequences were performed using Clustal
581 Omega, accessible through the European Bioinformatics Institute website
582 (https://www.ebi.ac.uk/Tools/msa/) using default parameters. The MSA output was analysed using
583 Jalview (78) to assess the presence of known rosetting motifs across rosetting and non-rosetting
584 variants. The sequence analysis included NTS-DBLα sequences from experimentally validated PfEMP1
585 variants, comprising 12 rosetting (Table 2) and 12 non-rosetting (Table 3) variants.

586 **Table 2: *var* genes encode rosetting PfEMP1 variants*.**

S/N	*var* gene/alternative name	Group**	DBLα class	DC	Ref.
1	*pc0053var_r1/9197var15*	A	1.2	15	This study
2	*pfke11var_r1/pfke11.g448*	A	1.2	15	This study
3	*pfke08var_r1/9605.g502*	A	1.8	11	This study
4	*pfke10var_r1/11019var1*	A	1.8	11	This study
5	*IT4var60*	A	1.8	11	(15)
6	*TM284var1*	A	1.8	11	(17)
7	*IT4var09*	A	1.6	16	(14)
8	*PaloAltovarO*	A	1.6	16	(32)
9	*3D7PF13_0003*	A	1.5	16	(16)
10	*HB3var06*	A	1.5	16	(17)
11	*Muz12var1*	A	1.5	16	(17)
12	*TM180var1*	B	2	8	(17)

587 *Parasite lines expressing these variants have been examined microscopically and shown to form rosettes and
588 evidence that the PfEMP1 NTS-DBLa binds erythrocytes has been provided.
589 ** Rask et al (27) or Otto et al (35).
590
591
592 **Table 3: *var* genes encode non-rosetting PfEMP1 variants*.**

S/N	*var* gene	Group**	DC	Associated phenotype	Ref.
1	*IT4var19*	B	8	HBEC-binding***	(49)
2	*3D7PFD0020c*	A	8	HBEC-binding	(49)
3	*pfke08var_r1/PFKE08.g501*	B	8	ICAM-1, EPCR	this study
5	*HB3var03*	A	13	HBEC-binding	(49)
6	*IT4var07*	A	13	HBEC-binding	(49)
7	*pc0053-C.g96/9197var5*	B	17	HBEC-binding	Rowe lab unpublished
8	*IT4var44*	B	12	Clumping	Rowe lab unpublished
9	*IT4var67*	B	12	Clumping	Rowe lab unpublished
10	*HB3var05*	A	16	Unknown	Rowe lab unpublished
11	*IT4var14*	B	14	CD36- and ICAM-1 binding	(79)
12	*IT4var16*	B	14	CD36- and ICAM-1 binding	(80)

593 *Parasite lines expressing these variants have been examined microscopically and no rosettes were seen.
594 ** Rask et al (27) or Otto et al (35).
595 *** HBEC, human brain endothelial cell
596

597 **CIDRα1.5 analysis methods**

598 The amino acid sequences of the all PFKE CIDRα1.5 domains were extracted based on previously
599 published domain boundaries (35). The sequences were aligned with default parameters using
600 MUSCLE (v3.8.1551) (81). IQTREE (v2.0.5) was then used to generate a maximum likelihood tree of
601 the aligned sequences (82). The IQTREE command "*iqtree2 --safe -s cidra.aa.aligned.fasta -m*
602 *JTT+F+I+I+R10 -alrt 1000*" was used and the results were visualised and annotated using ggtree in R
603 (73, 83).

604

605

606 **Acknowledgements**

607 This work was funded by the Wellcome Trust grant numbers 084226 (senior fellowship to JAR),
608 204052/Z/16/Z (PhD studentship to FM), 218492/Z/19/Z (PhD studentship to RL and BRO) and
609 203077/Z/16/Z (core Award to the KEMRI-Wellcome Trust Research Programme). The work is
610 published with the permission of the Director of KEMRI.

611

612

613
614
615

616

617

618

619 **References**

620 1. Lee WC, Russell B, Renia L. Evolving perspectives on rosetting in malaria. Trends Parasitol.
621 2022;38(10):882-9.

622 2. Rowe A, Obeiro J, Newbold CI, Marsh K. *Plasmodium falciparum* rosetting is associated with
623 malaria severity in Kenya. Infect Immun. 1995;63(6):2323-6.

624 3. Carlson J, Helmby H, Hill AV, Brewster D, Greenwood BM, Wahlgren M. Human cerebral
625 malaria: association with erythrocyte rosetting and lack of anti-rosetting antibodies. Lancet.
626 1990;336(8729):1457-60.

627 4. Normark J, Nilsson D, Ribacke U, Winter G, Moll K, Wheelock CE, et al. PfEMP1-DBL1alpha
628 amino acid motifs in severe disease states of *Plasmodium falciparum* malaria. Proc Natl Acad Sci U S
629 A. 2007;104(40):15835-40.

630 5. Doumbo OK, Thera MA, Kone AK, Raza A, Tempest LJ, Lyke KE, et al. High levels of *Plasmodium*
631 *falciparum* rosetting in all clinical forms of severe malaria in African children. American Journal of
632 Tropical Medicine and Hygiene. 2009;81(6):987-93.

633 6. Nash GB, Cooke BM, Carlson J, Wahlgren M. Rheological properties of rosettes formed by red
634 blood cells parasitized by *Plasmodium falciparum*. Br J Haematol. 1992;82(4):757-63.

635 7. Kaul DK, Roth EFJ, Nagel RL, Howard RJ, Handunnetti SM. Rosetting of *Plasmodium falciparum*-
636 infected red blood cells with uninfected red blood cells enhances microvascular obstruction under
637 flow conditions. Blood. 1991;78(3):812-9.

638 8. Chotivanich KT, Dondorp AM, White NJ, Peters K, Vreeken J, Kager PA, et al. The resistance to
639 physiological shear stresses of the erythrocytic rosettes formed by cells infected with *Plasmodium*
640 *falciparum*. Ann Trop Med Parasitol. 2000;94(3):219-26.

641 9. Jotten AM, Moll K, Wahlgren M, Wixforth A, Westerhausen C. Blood group and size dependent
642 stability of *P. falciparum* infected red blood cell aggregates in capillaries. Biomicrofluidics.
643 2020;14(2):024104.

644 10. Rowe JA, Handel IG, Thera MA, Deans AM, Lyke KE, Koné A, et al. Blood group O protects
645 against severe Plasmodium falciparum malaria through the mechanism of reduced rosetting. Proc Natl
646 Acad Sci U S A. 2007;104(44):17471-6.

647 11. Cockburn IA, Mackinnon MJ, O'Donnell A, Allen SJ, Moulds JM, Baisor M, et al. A human
648 complement receptor 1 polymorphism that reduces *Plasmodium falciparum* rosetting confers
649 protection against severe malaria. Proc Natl Acad Sci U S A. 2004;101(1):272-7.

650 12. Opi DH, Swann O, Macharia A, Uyoga S, Band G, Ndila CM, et al. Two complement receptor
651 one alleles have opposing associations with cerebral malaria and interact with α-thalassaemia. Elife.
652 2018;7.

653 13. Treutiger CJ, Carlson J, Scholander C, Wahlgren M. The time course of cytoadhesion,
654 immunoglobulin binding, rosette formation, and serum-induced agglutination of *Plasmodium*
655 *falciparum*-infected erythrocytes. Am J Trop Med Hyg. 1998;59(2):202-7.
656 14. Rowe JA, Moulds JM, Newbold CI, Miller LH. *P. falciparum* rosetting mediated by a parasite-
657 variant erythrocyte membrane protein and complement-receptor 1. Nature. 1997;388(6639):292-5.
658 15. Albrecht L, Moll K, Blomqvist K, Normark J, Chen Q, Wahlgren M. var gene transcription and
659 PfEMP1 expression in the rosetting and cytoadhesive *Plasmodium falciparum* clone FCR3S1.2. Malar
660 J. 2011;10:17.
661 16. Vigan-Womas I, Guillotte M, Juillerat A, Vallieres C, Lewit-Bentley A, Tall A, et al. Allelic
662 diversity of the *Plasmodium falciparum* erythrocyte membrane protein 1 entails variant-specific red
663 cell surface epitopes. PLoS One. 2011;6(1):e16544.
664 17. Ghumra A, Semblat JP, Ataide R, Kifude C, Adams Y, Claessens A, et al. Induction of strain-
665 transcending antibodies against Group A PfEMP1 surface antigens from virulent malaria parasites.
666 PLoS Pathog. 2012;8(4):e1002665.
667 18. Goel S, Palmkvist M, Moll K, Joannin N, Lara P, Akhouri RR, et al. RIFINs are adhesins implicated
668 in severe *Plasmodium falciparum* malaria. Nature Medicine. 2015;21(4):314-7.
669 19. Niang M, Bei AK, Madnani KG, Pelly S, Dankwa S, Kanjee U, et al. STEVOR is a *Plasmodium*
670 *falciparum* erythrocyte binding protein that mediates merozoite invasion and rosetting. Cell Host
671 Microbe. 2014;16(1):81-93.
672 20. Gardner MJ, Hall N, Fung E, White O, Berriman M, Hyman RW, et al. Genome sequence of the
673 human malaria parasite Plasmodium falciparum. Nature. 2002;419(6906):498-511.
674 21. Kyriacou HM, Stone GN, Challis RJ, Raza A, Lyke KE, Thera MA, et al. Differential var gene
675 transcription in Plasmodium falciparum isolates from patients with cerebral malaria compared to
676 hyperparasitaemia. Molecular and Biochemical Parasitology. 2006;150(2):211-8.
677 22. Lavstsen T, Turner L, Saguti F, Magistrado P, Rask TS, Jespersen JS, et al. Plasmodium
678 falciparum erythrocyte membrane protein 1 domain cassettes 8 and 13 are associated with severe
679 malaria in children. Proc Natl Acad Sci U S A. 2012;109(26):E1791-800.
680 23. Warimwe GM, Fegan G, Musyoki JN, Newton CR, Opiyo M, Githinji G, et al. Prognostic
681 indicators of life-threatening malaria are associated with distinct parasite variant antigen profiles. Sci
682 Transl Med. 2012;4(129):129ra45.
683 24. Bernabeu M, Danziger SA, Avril M, Vaz M, Babar PH, Brazier AJ, et al. Severe adult malaria is
684 associated with specific PfEMP1 adhesion types and high parasite biomass. Proc Natl Acad Sci U S A.
685 2016;113(23):E3270-9.

686 25. Jespersen JS, Wang CW, Mkumbaye SI, Minja DT, Petersen B, Turner L, et al. Plasmodium
687 falciparum var genes expressed in children with severe malaria encode CIDRalpha1 domains. EMBO
688 Mol Med. 2016;8(8):839-50.
689 26. Smith JD, Subramanian G, Gamain B, Baruch DI, Miller LH. Classification of adhesive domains
690 in the *Plasmodium falciparum* erythrocyte membrane protein 1 family. Molecular and Biochemical
691 Parasitology. 2000;110(2):293-310.
692 27. Rask TS, Hansen DA, Theander TG, Gorm Pedersen A, Lavstsen T. *Plasmodium falciparum*
693 erythrocyte membrane protein 1 diversity in seven genomes--divide and conquer. PLoS Comput Biol.
694 2010;6(9):e1000933.
695 28. Smith JD, Rowe JA, Higgins MK, Lavstsen T. Malaria's deadly grip: cytoadhesion of Plasmodium
696 falciparum-infected erythrocytes. Cell Microbiol. 2013;15(12):1976-83.
697 29. Hsieh FL, Turner L, Bolla JR, Robinson CV, Lavstsen T, Higgins MK. The structural basis for CD36
698 binding by the malaria parasite. Nat Commun. 2016;7:12837.
699 30. Lennartz F, Adams Y, Bengtsson A, Olsen RW, Turner L, Ndam NT, et al. Structure-Guided
700 Identification of a Family of Dual Receptor-Binding PfEMP1 that Is Associated with Cerebral Malaria.
701 Cell Host Microbe. 2017;21(3):403-14.
702 31. Lau CK, Turner L, Jespersen JS, Lowe ED, Petersen B, Wang CW, et al. Structural conservation
703 despite huge sequence diversity allows EPCR binding by the PfEMP1 family implicated in severe
704 childhood malaria. Cell Host Microbe. 2015;17(1):118-29.
705 32. Vigan-Womas I, Guillotte M, Le Scanf C, Igonet S, Petres S, Juillerat A, et al. An in vivo and in
706 vitro model of *Plasmodium falciparum* rosetting and autoagglutination mediated by varO, a group A
707 var gene encoding a frequent serotype. Infect Immun. 2008;76(12):5565-80.
708 33. Tan J, Pieper K, Piccoli L, Abdi A, Perez MF, Geiger R, et al. A LAIR1 insertion generates broadly
709 reactive antibodies against malaria variant antigens. Nature. 2016;529(7584):105-9.
710 34. Kioko M, Pance A, Mwangi S, Goulding D, Kemp A, Rono M, et al. Extracellular vesicles could
711 be a putative posttranscriptional regulatory mechanism that shapes intracellular RNA levels in
712 Plasmodium falciparum. Nat Commun. 2023;14(1):6447.
713 35. Otto TD, Assefa SA, Bohme U, Sanders MJ, Kwiatkowski D, Pf3k c, et al. Evolutionary analysis
714 of the most polymorphic gene family in falciparum malaria. Wellcome Open Res. 2019;4:193.
715 36. Peters JM, Fowler EV, Krause DR, Cheng Q, Gatton ML. Differential changes in *Plasmodium*
716 *falciparum var* transcription during adaptation to culture. J Infect Dis. 2007;195(5):748-55.
717 37. Ghumra A, Semblat JP, McIntosh RS, Raza A, Rasmussen IB, Braathen R, et al. Identification of
718 residues in the Cmu4 domain of polymeric IgM essential for interaction with *Plasmodium falciparum*
719 erythrocyte membrane protein 1 (PfEMP1). Journal of Immunology. 2008;181(3):1988-2000.

720 38. Stevenson L, Huda P, Jeppesen A, Laursen E, Rowe JA, Craig A, et al. Investigating the function
721 of F -specific binding of IgM to *Plasmodium falciparum* erythrocyte membrane protein 1 mediating
722 erythrocyte rosetting. Cell Microbiol. 2014.
723 39. Akhouri RR, Goel S, Furusho H, Skoglund U, Wahlgren M. Architecture of Human IgM in
724 Complex with *P. falciparum* Erythrocyte Membrane Protein 1. Cell Rep. 2016;14(4):723-36.
725 40. Heddini A, Pettersson F, Kai O, Shafi J, Obiero J, Chen Q, et al. Fresh isolates from children with
726 severe Plasmodium falciparum malaria bind to multiple receptors. Infect Immun. 2001;69(9):5849-56.
727 41. Rowe JA, Shafi J, Kai OK, Marsh K, Raza A. Nonimmune IgM, but not IgG binds to the surface
728 of *Plasmodium falciparum*-infected erythrocytes and correlates with rosetting and severe malaria.
729 American Journal of Tropical Medicine and Hygiene. 2002;66(6):692-9.
730 42. Stevenson L, Laursen E, Cowan GJ, Bandoh B, Barfod L, Cavanagh DR, et al. α2-Macroglobulin
731 Can Crosslink Multiple *Plasmodium falciparum* Erythrocyte Membrane Protein 1 (PfEMP1) Molecules
732 and May Facilitate Adhesion of Parasitized Erythrocytes. PLoS Pathog. 2015;11(7):e1005022.
733 43. Leech JH, Barnwell JW, Miller LH, Howard RJ. Identification of a strain-specific malarial antigen
734 exposed on the surface of *Plasmodium falciparum* infected erythrocytes. J Exp Med. 1984;159:1567-
735 75.
736 44. Kyes SA, Rowe JA, Kriek N, Newbold CI. Rifins: a second family of clonally variant proteins
737 expressed on the surface of red cells infected with *Plasmodium falciparum*. Proc Natl Acad Sci U S A.
738 1999;96(16):9333-8.
739 45. Fernandez V, Hommel M, Chen Q, Hagblom P, Wahlgren M. Small, clonally variant antigens
740 expressed on the surface of the *Plasmodium falciparum*-infected erythrocyte are encoded by the rif
741 gene family and are the target of human immune responses. J Exp Med. 1999;190(10):1393-404.
742 46. Bull PC, Berriman M, Kyes S, Quail MA, Hall N, Kortok MM, et al. *Plasmodium falciparum*
743 Variant Surface Antigen Expression Patterns during Malaria. PLoS Pathog. 2005;1(3):e26.
744 47. Turner L, Lavstsen T, Berger SS, Wang CW, Petersen JE, Avril M, et al. Severe malaria is
745 associated with parasite binding to endothelial protein C receptor. Nature. 2013;498(7455):502-5.
746 48. Ghumra A, Khunrae P, Ataide R, Raza A, Rogerson SJ, Higgins MK, et al. Immunisation with
747 recombinant PfEMP1 domains elicits functional rosette-inhibiting and phagocytosis-inducing
748 antibodies to *Plasmodium falciparum*. PLoS One. 2011;6(1):e16414.
749 49. Claessens A, Adams Y, Ghumra A, Lindergard G, Buchan CC, Andisi C, et al. A subset of group
750 A-like *var* genes encodes the malaria parasite ligands for binding to human brain endothelial cells.
751 Proc Natl Acad Sci U S A. 2012;109:E1772-81.

752 50. Voss TS, Healer J, Marty AJ, Duffy MF, Thompson JK, Beeson JG, et al. A var gene promoter
753 controls allelic exclusion of virulence genes in Plasmodium falciparum malaria. Nature.
754 2006;439(7079):1004-8.
755 51. Joergensen L, Bengtsson DC, Bengtsson A, Ronander E, Berger SS, Turner L, et al. Surface co-
756 expression of two different PfEMP1 antigens on single plasmodium falciparum-infected erythrocytes
757 facilitates binding to ICAM1 and PECAM1. PLoS Pathog. 2010;6(9):e1001083.
758 52. Vigan-Womas I, Guillotte M, Juillerat A, Hessel A, Raynal B, England P, et al. Structural basis
759 for the ABO blood-group dependence of *Plasmodium falciparum* rosetting. PLoS Pathog.
760 2012;8(7):e1002781.
761 53. Ji C, Shen H, Su C, Li Y, Chen S, Sharp TH, et al. Plasmodium falciparum has evolved multiple
762 mechanisms to hijack human immunoglobulin M. Nat Commun. 2023;14(1):2650.
763 54. Handunnetti SM, Hasler TH, Howard RJ. *Plasmodium falciparum*-infected erythrocytes do not
764 adhere well to C32 melanoma cells or CD36 unless rosettes with uninfected erythrocytes are first
765 disrupted. Infect Immun. 1992;60(3):928-32.
766 55. Rorick MM, Baskerville EB, Rask TS, Day KP, Pascual M. Identifying functional groups among
767 the diverse, recombining antigenic var genes of the malaria parasite Plasmodium falciparum from a
768 local community in Ghana. PLoS Comput Biol. 2018;14(6):e1006174.
769 56. McQuaid F, Rowe JA. Rosetting revisited: a critical look at the evidence for host erythrocyte
770 receptors in Plasmodium falciparum rosetting. Parasitology. 2020;147(1):1-11.
771 57. Deb B, Das A, Vilvadrinath R, Jangra A, Shukla MS, Akhouri RR, et al. Glycophorin B-PfEMP1
772 interaction mediates robust rosetting in Plasmodium falciparum. Int J Biol Macromol. 2024;262(Pt
773 1):129868.
774 58. Le Scanf C, Vigan-Womas I, Contamin H, Guillotte M, Bischoff E, Mercereau-Puijalon O.
775 Rosetting is associated with increased Plasmodium falciparum in vivo multiplication rate in the Saimiri
776 sciureus monkey. Microbes Infect. 2008;10(4):447-51.
777 59. Mackinnon MJ, Read AF. Genetic relationships between parasite virulence and transmission
778 in the rodent malaria *Plasmodium chabaudi*. Evolution. 1999;54:689-703.
779 60. Clough B, Atilola FA, Pasvol G. The role of rosetting in the multiplication of *Plasmodium*
780 *falciparum*: rosette formation neither enhances nor targets parasite invasion into uninfected red cells.
781 Brit J Haematol. 1998;100(1):99-104.
782 61. Deans AM, Rowe JA. Plasmodium falciparum: Rosettes do not protect merozoites from
783 invasion-inhibitory antibodies. Experimental Parasitol. 2006;112(4):269-73.

784 62. Moll K, Palmkvist M, Ch'ng J, Kiwuwa MS, Wahlgren M. Evasion of Immunity to Plasmodium
785 falciparum: Rosettes of Blood Group A Impair Recognition of PfEMP1. PLoS One.
786 2015;10(12):e0145120.
787 63. Magallon-Tejada A, Machevo S, Cistero P, Lavstsen T, Aide P, Rubio M, et al. Cytoadhesion to
788 gC1qR through Plasmodium falciparum Erythrocyte Membrane Protein 1 in Severe Malaria. PLoS
789 Pathog. 2016;12(11):e1006011.
790 64. Wichers JS, Tonkin-Hill G, Thye T, Krumkamp R, Kreuels B, Strauss J, et al. Common virulence
791 gene expression in adult first-time infected malaria patients and severe cases. Elife. 2021;10.
792 65. Dondorp AM, Pongponratn E, White NJ. Reduced microcirculatory flow in severe falciparum
793 malaria: pathophysiology and electron-microscopic pathology. Acta Trop. 2004;89(3):309-17.
794 66. Barrera V, MacCormick IJC, Czanner G, Hiscott PS, White VA, Craig AG, et al. Neurovascular
795 sequestration in paediatric P. falciparum malaria is visible clinically in the retina. Elife. 2018;7.
796 67. Ben Abderrahim S, Gharsallaoui S, Ben Daly A, Mosbahi A, Chaieb S, Nfikha Z, et al. Imported
797 malaria in adults: about a case of cerebral malaria. Egypt J Forensic Sci. 2022;12(1):19.
798 68. Vogt AM, Barragan A, Chen Q, Kironde F, Spillmann D, Wahlgren M. Heparan sulfate on
799 endothelial cells mediates the binding of Plasmodium falciparum-infected erythrocytes via the
800 DBL1alpha domain of PfEMP1. Blood. 2003;101(6):2405-11.
801 69. Adams Y, Kuhnrae P, Higgins MK, Ghumra A, Rowe JA. Rosetting *Plasmodium falciparum*-
802 infected erythrocytes bind to human brain microvascular endothelial cells in vitro, demonstrating a
803 dual adhesion phenotype mediated by distinct *P. falciparum* erythrocyte membrane protein 1
804 domains. Infect Immun. 2014;82(3):949-59.
805 70. Scherf A, Hernandez-Rivas R, Buffet P, Bottius E, Benatar C, Pouvelle B, et al. Antigenic
806 variation in malaria: in situ switching, relaxed and mutually exclusive transcription of var genes during
807 intra-erythrocytic development in Plasmodium falciparum. EMBO J. 1998;17(18):5418-26.
808 71. McLean FE, Azasi Y, Sutherland C, Toboh E, Ansong D, Agbenyega T, et al. Detection of
809 naturally acquired, strain-transcending antibodies against rosetting Plasmodium falciparum strains in
810 humans. Infect Immun. 2024:e0001524.
811 72. Handunnetti SM, Gilladoga AD, van Schravendijk MR, Nakamura K, Aikawa M, Howard RJ.
812 Purification and in vitro selection of rosette-positive (R+) and rosette-negative (R-) phenotypes of
813 knob-positive *Plasmodium falciparum* parasites. Am J Trop Med Hyg. 1992;46(4):371-81.
814 73. R Core Team. R: A Language and Environment for Statistical Computing. R Foundation for
815 Statistical Computing; 2022.
816 74. Altschul SF, Gish W, Miller W, Myers EW, Lipman DJ. Basic local alignment search tool. J Mol
817 Biol. 1990;215(3):403-10.

818 75. Kraemer SM, Gupta L, Smith JD. New tools to identify var sequence tags and clone full-length
819 genes using type-specific primers to Duffy binding-like domains. Mol Biochem Parasitol.
820 2003;129(1):91-102.
821 76. Higgins MK. Overproduction, purification and crystallization of a chondroitin sulfate A-binding
822 DBL domain from a Plasmodium falciparum var2csa-encoded PfEMP1 protein. Acta Crystallogr Sect F
823 Struct Biol Cryst Commun. 2008;64(Pt 3):221-3.
824 77. Angeletti D, Sandalova T, Wahlgren M, Achour A. Binding of subdomains 1/2 of PfEMP1-
825 DBL1alpha to heparan sulfate or heparin mediates Plasmodium falciparum rosetting. PLoS One.
826 2015;10(3):e0118898.
827 78. Waterhouse AM, Procter JB, Martin DM, Clamp M, Barton GJ. Jalview Version 2--a multiple
828 sequence alignment editor and analysis workbench. Bioinformatics. 2009;25(9):1189-91.
829 79. Janes JH, Wang CP, Levin-Edens E, Vigan-Womas I, Guillotte M, Melcher M, et al. Investigating
830 the Host Binding Signature on the Plasmodium falciparum PfEMP1 Protein Family. PLoS Pathog.
831 2011;7(5):e1002032.
832 80. Avril M, Tripathi AK, Brazier AJ, Andisi C, Janes JH, Soma VL, et al. A restricted subset of var
833 genes mediates adherence of Plasmodium falciparum-infected erythrocytes to brain endothelial cells.
834 Proc Natl Acad Sci U S A. 2012;109(26):E1782-90.
835 81. Edgar RC. MUSCLE: multiple sequence alignment with high accuracy and high throughput.
836 Nucleic Acids Res. 2004;32(5):1792-7.
837 82. Nguyen LT, Schmidt HA, von Haeseler A, Minh BQ. IQ-TREE: a fast and effective stochastic
838 algorithm for estimating maximum-likelihood phylogenies. Mol Biol Evol. 2015;32(1):268-74.
839 83. Yu G, Smith DK, Zhu H, Guan Y, Lam TT-Y. ggtree: an r package for visualization and annotation
840 of phylogenetic trees with their covariates and other associated data. Methods Ecol Evol.
841 2017;8(1):28-36.
842

843

844 **A**

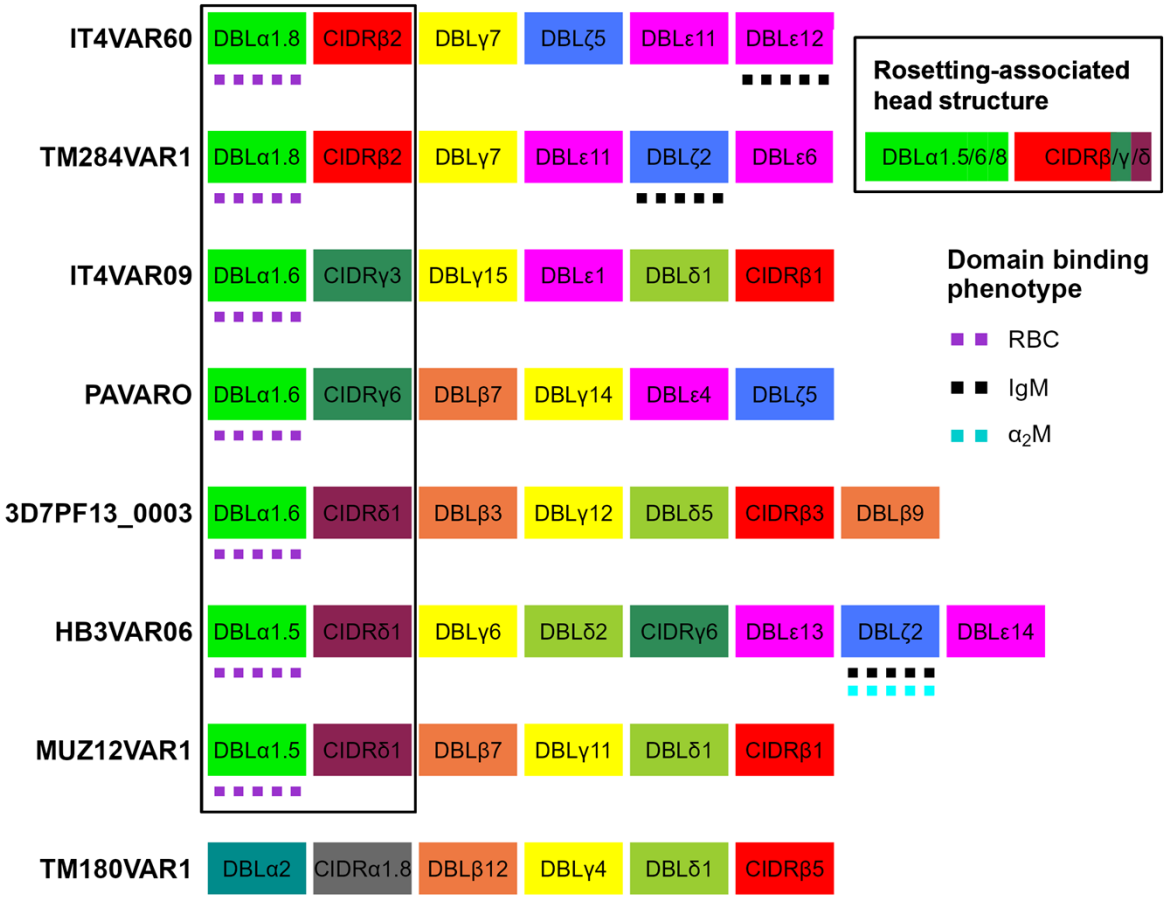

845

846 **B**

847
848
849
850 **Figure 1. Known rosette-mediating PfEMP1 variants and associated domain cassettes.** A) Diagram of
851 the PfEMP1 domain architecture of known rosette-mediating variants (14-17). The rosetting-
852 associated head structure, DBLα1.5/6/8-CIDRβ/γ/δ, is boxed. Domains that bind erythrocytes (RBC)
853 or serum proteins (IgM and α2M) are indicated. **B)** Diagram of domain cassettes (DCs) [as described
854 by (27)] which are relevant to the rosetting PfEMP1 variants characterised previously.

855
856

858 **A**

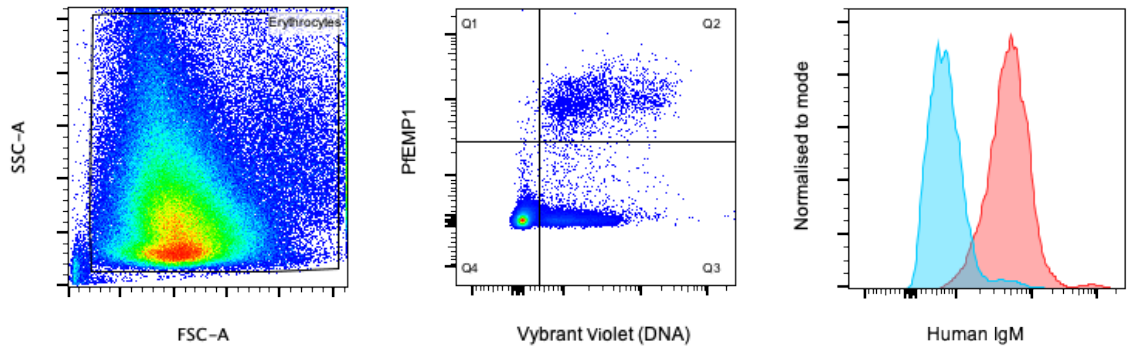

859

860 **B**

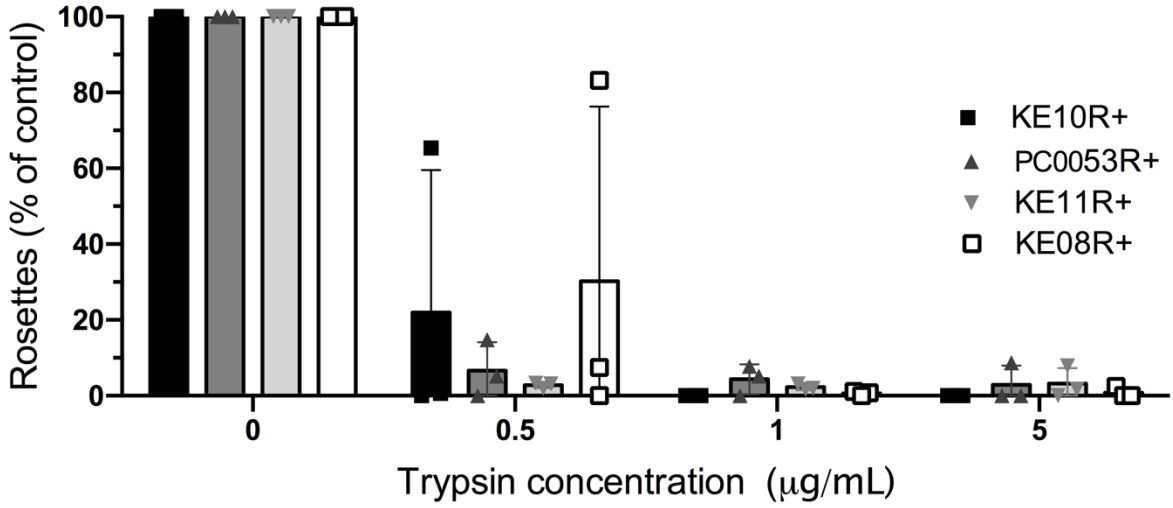

861
862

863 **Figure 2. Properties of the new Kenyan rosetting lines.** A) IgM binding by KE10R+ infected
864 erythrocytes detected by flow cytometry. Forward and side scatter were used to gate on erythrocytes
865 and exclude debris (left panel) and KE10VAR_R1-expressing infected erythrocytes were detected by
866 staining with 20μg/ml of polyclonal rabbit IgG against NTS-DBLα followed by 1/1000 dilution of Alexa
867 Fluor 647-conjugated goat anti-rabbit IgG secondary antibody and 1/2500 dilution of Vybrant
868 DyeCycle Violet (middle panel Q2). IgM staining of the Q2 cell population was detected with 1/1000
869 dilution of an Alexa Fluor 488-conjugated goat anti-human IgM heavy chain antibody (red). The
870 negative control (blue) was parasites grown in IgM-depleted medium and stained with the same
871 antibodies. Results are representative of two independent experiments. B) Effect of low-dose
872 trypsinisation on rosetting. Purified infected erythrocytes were treated with 0.5, 1 or 5 μg/ml of
873 trypsin for 5 mins and the rosette frequency relative to a control sample with no added enzyme was
874 calculated. The mean and standard deviation from three independent experiments per parasite line
875 is shown. The rosette frequency of the untreated controls was between 46%-81% (KE10R+), 45%-89%
876 (PC0053R+), 16%-30% (KE11R+) and 61%-91% (KE08R+).

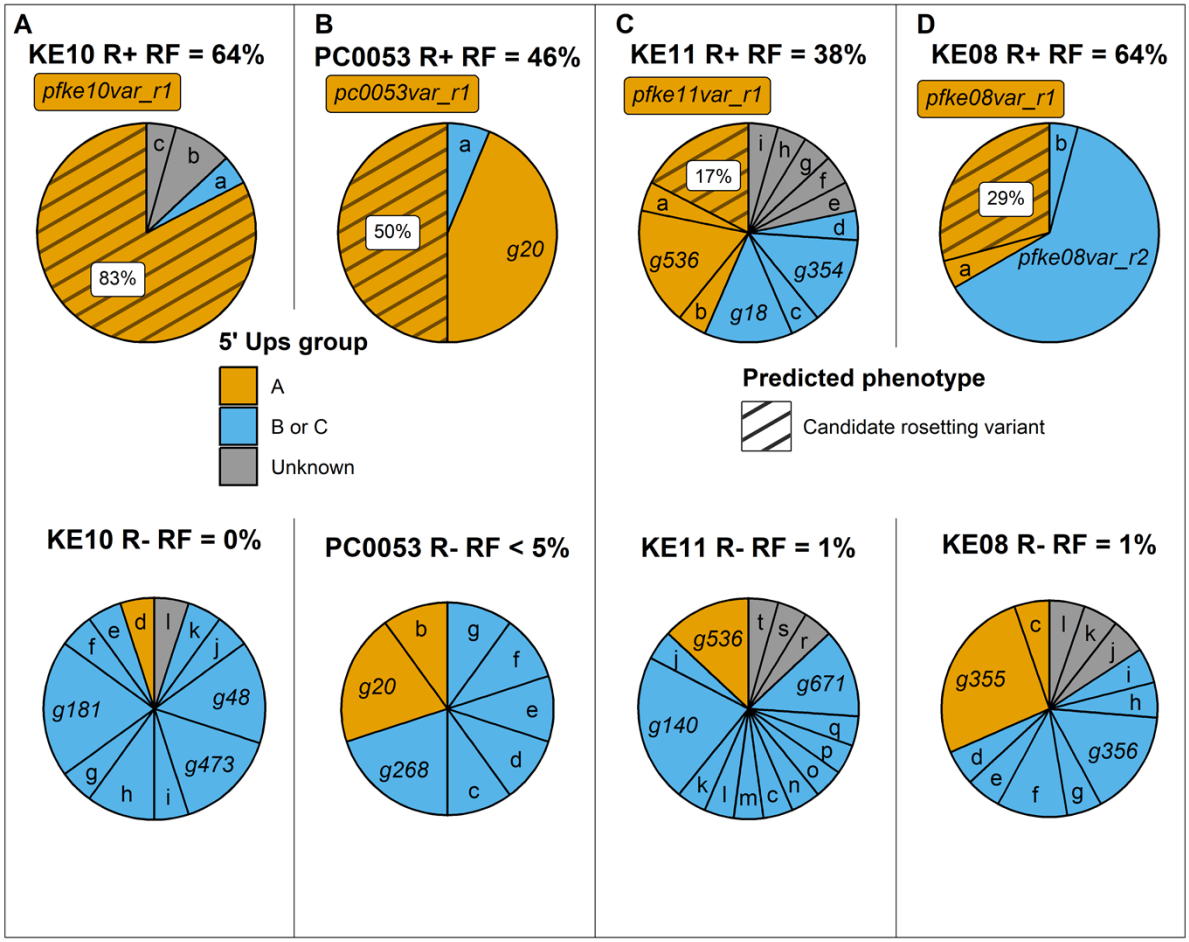

Figure 3. DBLα expression tag profiling of the new Kenyan rosetting lines. DBLα tag expression profiles showing the proportion each gene tag contributed to the overall expressed tag profile for each parasite population. *var* gene tags encoding candidate rosetting variants (hatched; percentage of all tags given in white box) are identified as predominant genes expressed in R+ parasites but not/rarely in isogenic R- parasites. Other large pie slices are identified by gene (g) number for each parasite line, and small slices are given letters, with the full information for each gene given in Supplementary Table 1. *var* gene groups are identified by colour. Slices labelled as "unknown" are from sequence tags that did not map back to an assembled *var* gene in that parasite's repertoire (34). The rosette frequency (RF) in the cycle in which the RNA was collected is shown for each parasite line. Results are representative of two independent experiments.

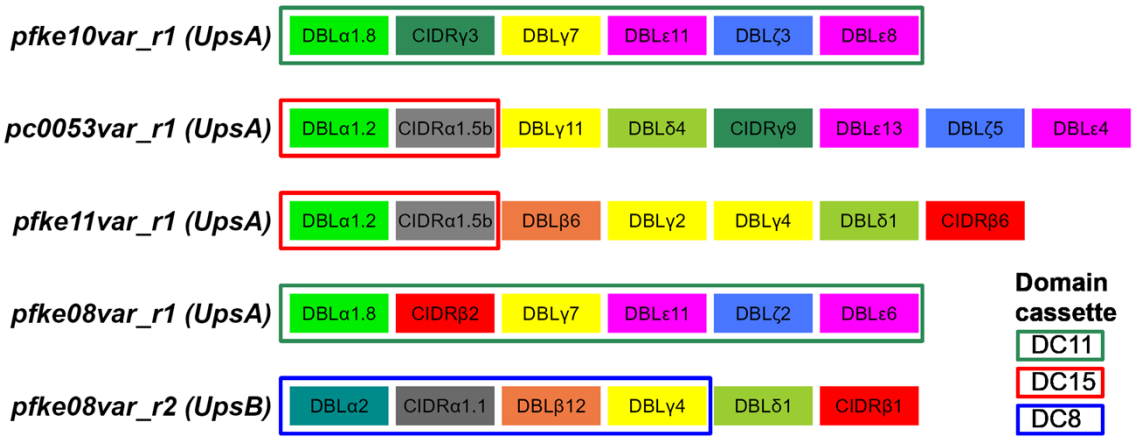

Figure 4. Domain architecture of the candidate rosette-mediating PfEMP1 variants. Domain cassettes are as described by Rask et al (27). The alternative names for these genes in the Pf3k database (34) are as follows: *pfke10var_r1/PX0203.g54; pc0053var_r1/PC0053-C.g687; pfke11var_r1/ PFKE11.g448 ; pfke08var_r1/ PFKE08.g502; pfke08var_r2/ PFKE08.g501.*

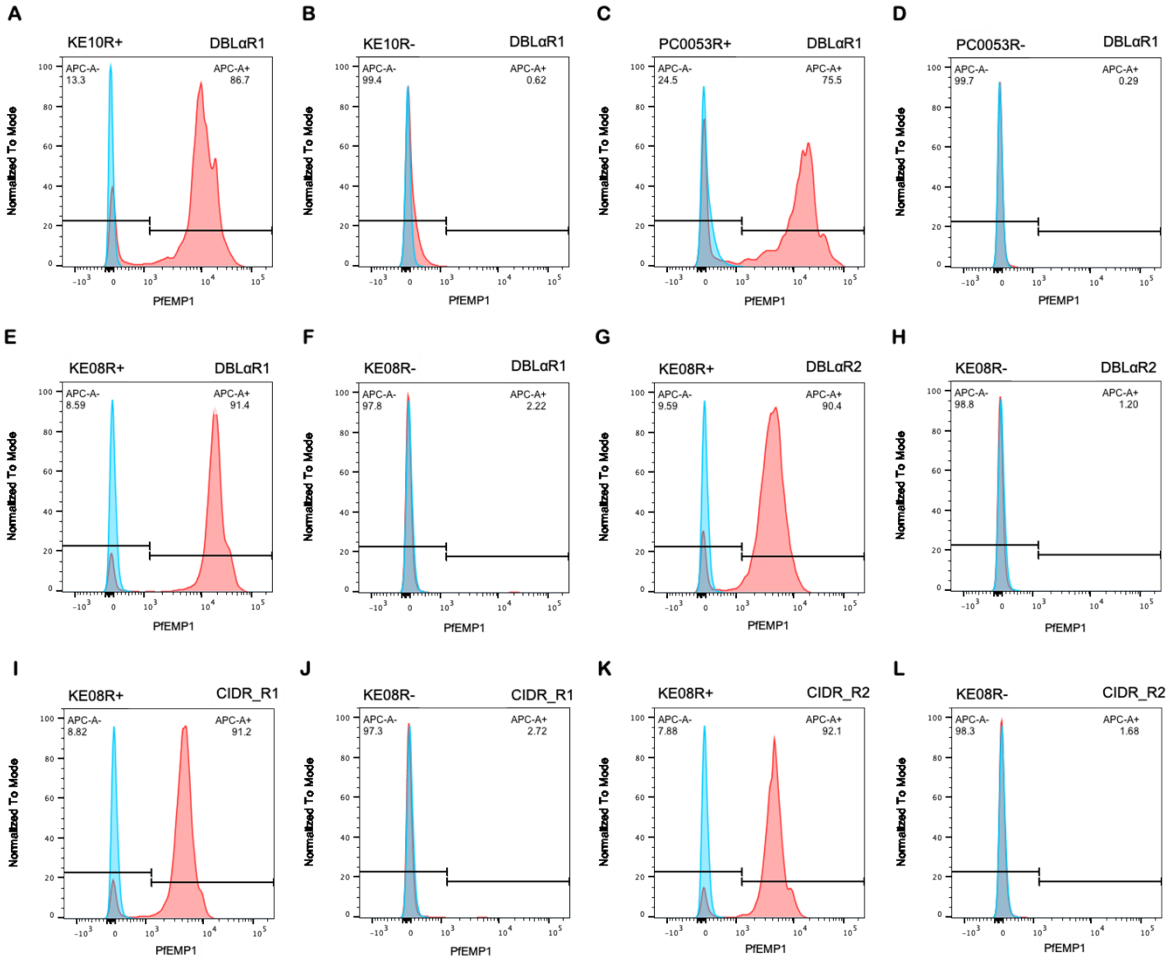

Figure 5. Staining of the surface of live infected erythrocytes with PfEMP1 antibodies. Fluorescence intensity histograms of rosetting (R+) and non-rosetting (R-) parasite lines stained with rabbit IgG against rosetting PfEMP1 variants (red) or negative control rabbit IgG against the NTS-DBLα domain of an irrelevant PfEMP1 variant (HB3VAR03, blue). A) parasite line KE10R+ with antibodies to KE10VAR_R1 NTS-DBLα. B) parasite line KE10R- with antibodies to KE10VAR_R1 NTS-DBLα. C) parasite line PC0053R+ with antibodies to PC0053VAR_R1 NTS-DBLα. D) parasite line PC0053R- with antibodies to PC0053VAR_R1 NTS-DBLα. E) parasite line KE08R+ with antibodies to KE08VAR_R1 NTS-DBLα. F) parasite line KE08R- with antibodies to KE08VAR_R1 NTS-DBLα. G) parasite line KE08R+ with antibodies to KE08VAR_R2 NTS-DBLα. H) parasite line KE08R- with antibodies to KE08VAR_R2 NTS-DBLα. I) parasite line KE08R+ with antibodies to KE08VAR_R1 CIDR. J) parasite line KE08R- with antibodies to KE08VAR_R1 CIDR. K) parasite line KE08R+ with antibodies to KE08VAR_R3 CIDR. L) parasite line KE08R- with antibodies to KE08VAR_R2 CIDR. PfEMP1 was detected with 20μg/ml rabbit IgG against PfEMP1 and 1/1000 dilution of Alexa Fluor 647-conjugated goat anti-rabbit IgG secondary antibody. Gates shows the percentage of mature infected erythrocytes positive for the variant. The rosette frequency at the time of staining was 70-90% for the R+ lines and <2% for the R- lines, and the percentage of positive staining infected erythrocytes (APC-A+, top right corner of each histogram)

closely matched the rosette frequency in each parasite line. Results are representative of at least two experiments for each parasite line.

943

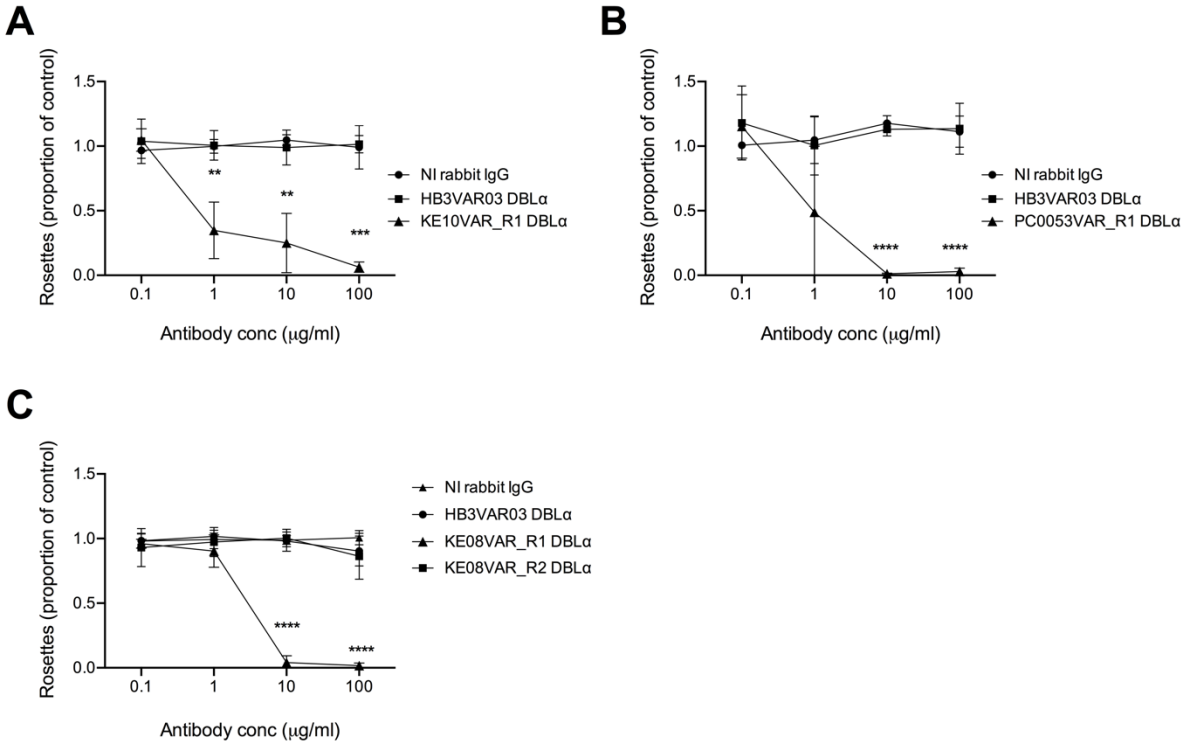

944
945

946 **Figure 6. Rosette disruption with rabbit IgG raised against candidate rosetting PfEMP1 variants.**
947 Antibodies to the candidate rosette-mediating PfEMP1 variant NTS-DBLα domains were tested in
948 rosette-disruption assays over a range of concentrations from 0.1-100 μg/mL. The rosette frequency
949 in the presence of antibody is shown as the proportion of the control value with no added antibody.
950 IgG from a non-immunised (NI) rabbit and from a rabbit immunised with the NTS-DBLα domain of a
951 non-rosetting PfEMP1 variant HB3VAR03 were used as negative controls in all experiments. Data
952 represent three independent experiments with the mean and standard deviation of the three
953 experiments shown. A) parasite line KE10R+; the rosette frequency of the no antibody control ranged
954 from 71%-87%. B) Parasite line PC0053R+; the rosette frequency of the no antibody control ranged
955 from 49%-60%. C) Parasite line KE08R+; the rosette frequency of the no antibody control ranged from
956 69%-92%. Data were analyzed by two-tailed paired t tests corrected for multiple comparisons with
957 the Holm-Sidak method ** $P<0.01$, *** $P<0.001$, **** $P<0.0001$.

958
959

960 **A**

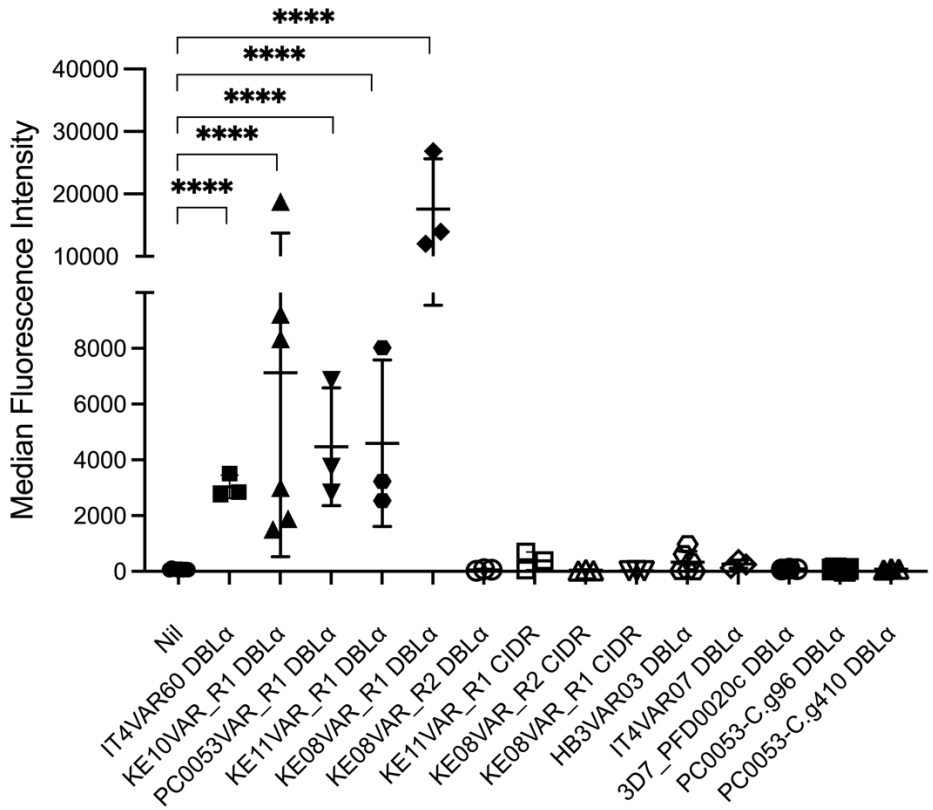

961

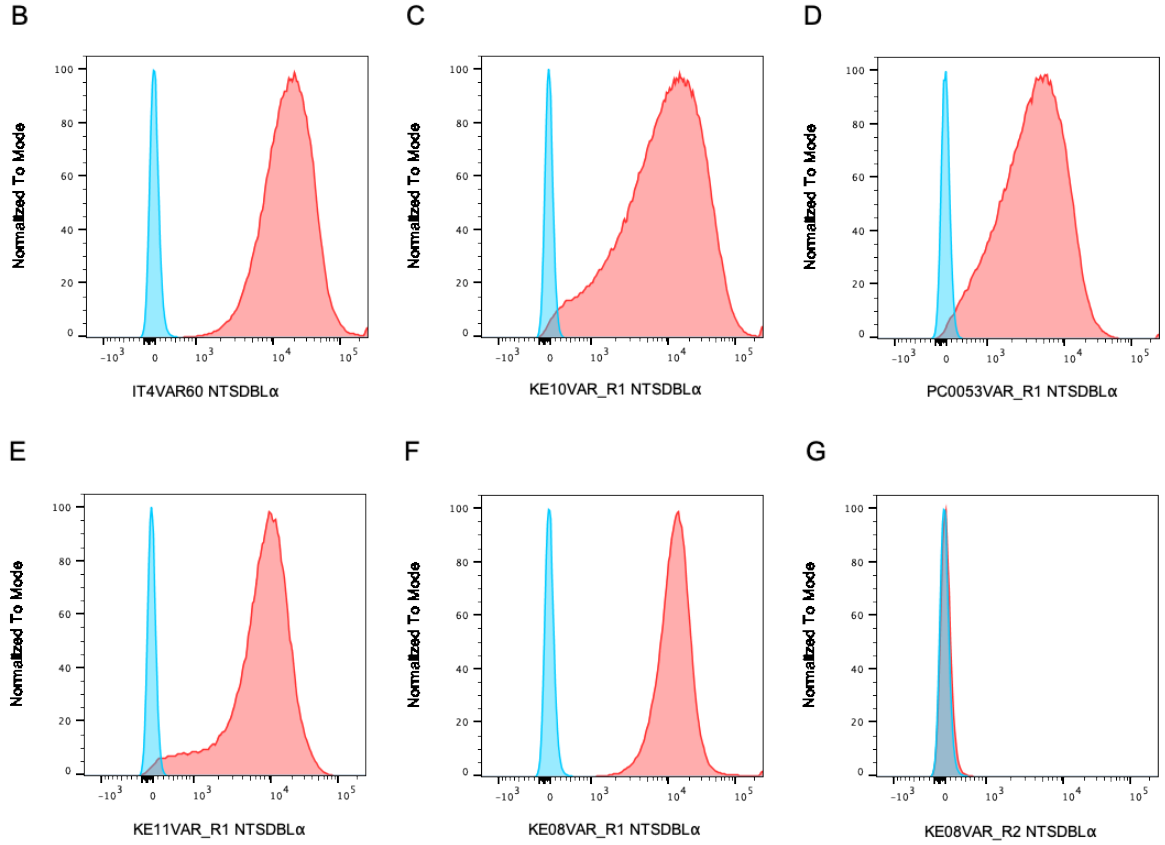

962
963 **Figure 7. Binding of PfEMP1 recombinant proteins to erythrocytes.** A) Recombinant proteins were
964 incubated with uninfected erythrocytes and bound protein detected with specific antibodies to each

965 domain. The positive control was the NTS-DBLα domain of the well-characterised rosetting variant
966 IT4var60 (15, 17) and negative controls were the NTS-DBLα domains from human brain endothelial
967 cell binding PfEMP1 variants HB3VAR03 (PFHB3_130080100), IT4VAR07 (PFIT_060036700),
968 3D7_PFD0020c (PF3D7_0400400), PC0053-C.g96 and PC0053-C.g410 that are known to be non-
969 rosetting (reference 48) and JA Rowe unpublished data). The mean and standard deviation of the
970 Alexa Fluor 488 median fluorescence intensity from at least three independent experiments per
971 protein is indicated. Data were log transformed and analysed by one way ANOVA with Dunnett's
972 multiple comparisons test compared to the "Nil" (no added protein) control. **** P<0.0001. B-G)
973 Example Alexa Fluor 488 fluorescence intensity histograms of recombinant PfEMP1 domains bound
974 to erythrocytes and detected by indirect immunofluorescence (red) compared to a non-rosetting NTS-
975 DBLα domain negative control (blue). The domain tested is indicated below each histogram.
976
977
978

979
980
981
982
983

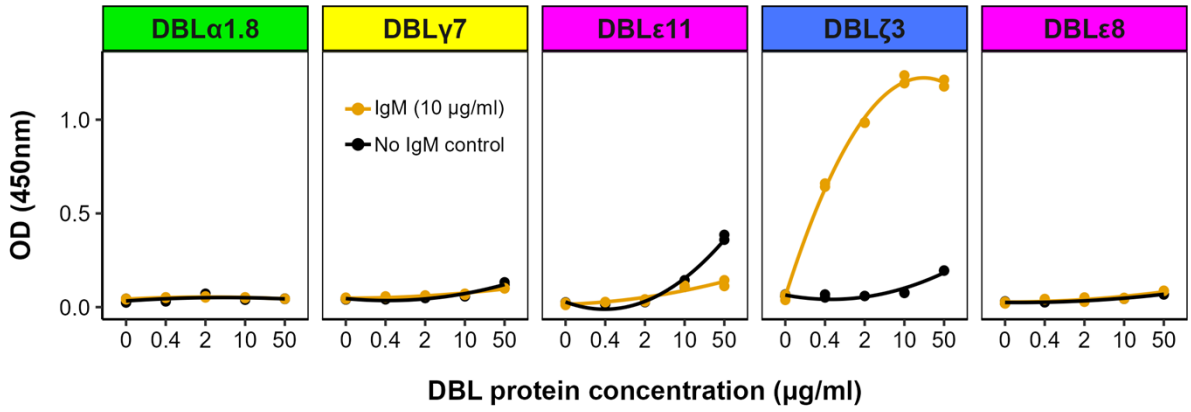

984
985
986

987 **Figure 8**. **The DBLζ3 domain of PFKE10VAR_R1 binds human IgM.** IgM was coated onto the wells of
988 an ELISA plate and individual PfEMP1 recombinant protein domains were added at four different 5-
989 fold dilutions. Wells with no IgM were included as negative controls. Binding was detected using an
990 HRP-conjugated anti-his tag antibody with TMB substrate and the absorbance read at 450nm. The
991 domains are shown from N- to C-terminal and the panels are colour-coded as previously described
992 (27). One representative experiment is shown out of at least two performed for each domain.
993

994

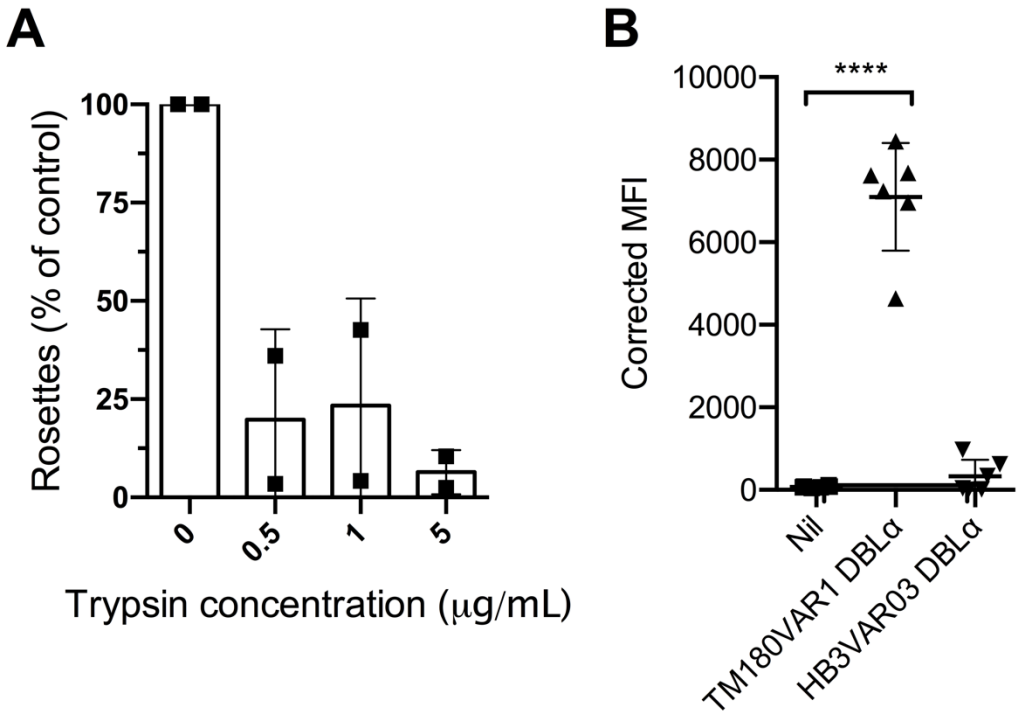

995
996
997 **Figure 9. The NTS-DBLα domain of TM180VAR1 mediates rosetting.** A) Effect of low dose
998 trypsinisation on TM180R^{+}. Infected erythrocytes were treated with 0.5, 1 or 5 μg/ml of trypsin for 5
999 mins in each experiment and the rosette frequency relative to a control sample with no added enzyme
1000 was calculated**.** Data represent two independent experiments with the mean indicated by bar height
1001 and the standard deviation shown. The rosette frequency in the untreated controls were 72% and
1002 61% respectively. B) Corrected Median Fluorescence Intensities (MFI) of uninfected erythrocytes in
1003 binding experiments with recombinant TM180VAR1 NTS-DBLα and the negative control HB3VAR03
1004 NTS-DBLα compared to "Nil" no added protein control. Data are from six independent experiments
1005 and the mean and standard deviation are shown. Significant differences by one-way ANOVA with
1006 Dunnett's multiple comparisons test compared to the "Nil" negative control are indicated.
1007 ****P<0.0001.
1008
1009
1010
1011
1012
1013
1014
1015
1016
1017
1018

1019
1020
1021
1022

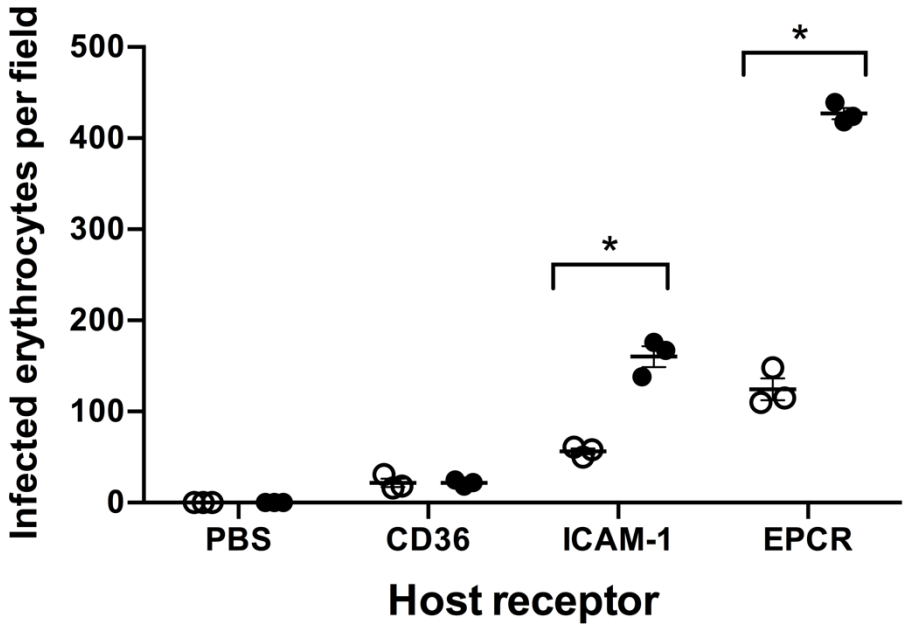

1023
1024
1025
1026 **Figure 10. Spot binding assay of KE08R+ to endothelial cell receptor proteins.** Adhesion of KE08R+
1027 infected erythrocytes to recombinant host receptor proteins was determined with (black circles) and
1028 without (white circles) prior rosette disruption with antibodies to KE08VAR_R1 NTS-DBLα. The
1029 number of infected erythrocytes bound per field was determined using an inverted microscope with
1030 a 40X objective and six fields were counted per spot in each experiment. The difference in mean
1031 binding values compared with the same receptor in the presence and absence of rosette from n=3
1032 independent experiments was analyzed by two-tailed paired t tests corrected for multiple
1033 comparisons with the Holm-Sidak method. *P< 0.05.

1034
1035
1036

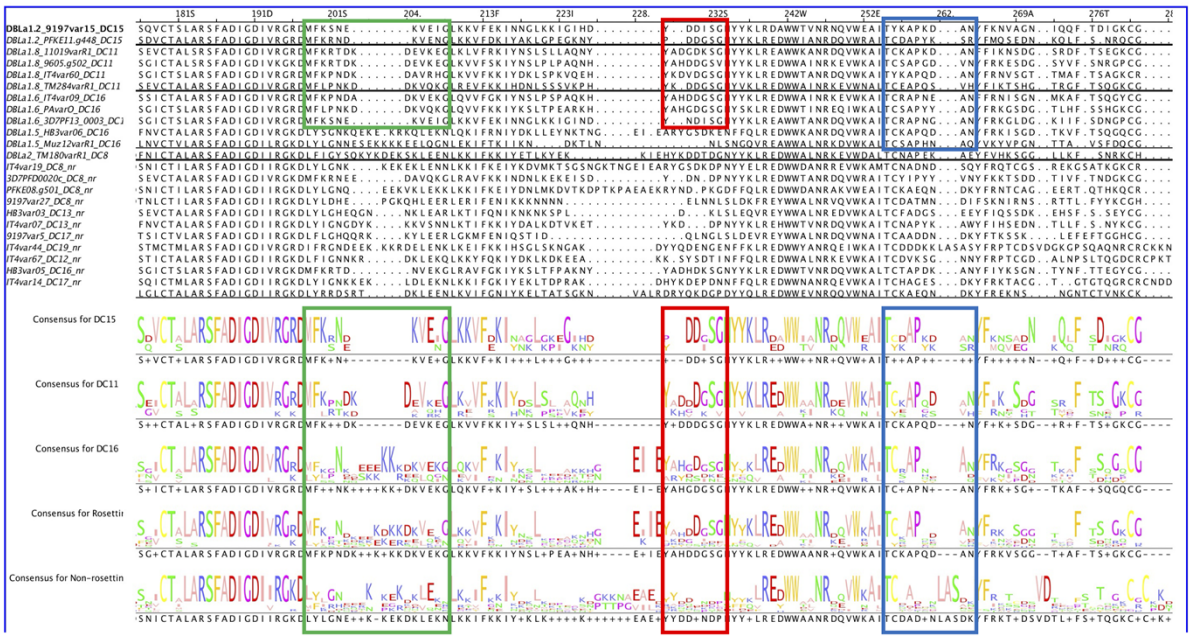

Figure 11. Rosetting motifs. The NTS-DBLα amino acid sequences from known rosetting (upper) and non-rosetting (lower) sequences were aligned in Jalview and amino acid motifs over-represented in the rosetting variants are shown in green, red and blue boxes.